2020

Virtual Impedance Based Decentralized Control for a Microgrid System

Ramkrishna Mishan
Minnesota State University, Mankato

Virtual Impedance Based Decentralized Control for a Microgrid System

By

Ramkrishna Mishan

A Thesis Submitted in Partial Fulfillment of the

Requirements for the Degree of

Master of Science

In

Electrical and Electronics Engineering

Major: Electrical Engineering

Minnesota State University, Mankato

Mankato, Minnesota

December 2020

December 11, 2020

Virtual Impedance Based Decentralized Control for a Microgrid System.

Mishan, Ramkrishna

This thesis has been examined and approved by the following members of the student's committee.

Dr. Jianwu Zeng
Advisor

Dr. Qiang Ye
Committee Member

Dr. Du'a Alzaleq
Committee Member

ACKNOWLEDGMENT

First and foremost, I want to show my gratitude to Dr. Jianwu Zeng for his ongoing assistance in my research and his persistence, motivation, enthusiasm, and immense knowledge in power system control. I could not ask for a better advisor and supervisor. He helped me to understand the realm of the microgrid control system. He advised me from time to time. Without him, it would be impossible to go through this journey. Then, I would like to thank my committee members: Dr. Qiang Ye and Dr. Du'a Alzaleq. Thanks for their time and effort to become one of my committee members and for their constructive criticism. I also want to thank my fellow lab mate members Xia Du, Dianzhi Yu, and Ning Jiahong, for simulating both hardware and Simulink, MATLAB.

I want to dispatch my profound appreciation to Minnesota State University, Mankato, to give me the opportunity to attend the graduate program. I want to express my sincere thanks to the electrical and electronics engineering department of MNSU to help me with the equipment and electrical devices to perform the research hardware simulation.

Finally, I convey my deepest gratitude to my parents and wife (Mrs. Rakhi Mondal) for their genuine love and support in my personal life. Without their backing, I would not be able to conduct my master's and research works.

Table of Contents

List of Abbreviations

DG: distributed generation

MG: micro grid

RESs: renewable energy sources

ESSs: energy storage systems

PV: photovoltaic

AC: alternating current

DC: direct current

LF: loop filter

LPF: low-pass filter

PCC: point of common coupling

PD: phase detection

PLL: phase-locked loop

PWM: pulse-width modulation

RMS: the root mean square

THD: total harmonic distortion

VCO: voltage-controlled oscillator

WT: wind turbine

TSR: tip-speed ratio

MPPT: maximum power point tracker

VSI: voltage source inerter

BESS: battery energy storage system

VF: voltage frequency

PQ: active reactive power

MT: micro turbine

SVPW: space vector pulse width modulation

FC: fuel cell

PI: proportional-integral

MPC: mode predictive controller

AGC: automatic generation control

MAS: multi agent system

Table of figures

Abstract

As greenhouse gases produced from the conventional power plant causes global climate change, using renewable energy sources (RESs) in the future power system is inevitable. To minimize greenhouse gases emission, the interest in renewable grid or micro-grid is growing nowadays. In the microgrid, especially in AC microgrids, converters play an important role in many areas, including microgrid integration, uninterrupted power supply, and flexible alternating current transmission systems. Inverter plays an essential role in grid integration because it serves the interface between the energy source and the power grid. The important aspect of the inverter is control.

This thesis studies several control strategies for the microgrid in both islanded and grid-connected modes while considering the intermittency of demand power and RESs. Generally, there are two types of control strategies: centralized control, the other is decentralized control. Decentralize control schemes are robust compare to other control systems and require low bandwidth e.g., only the nearest neighbor information is required.

Droop control, one of the conventional decentralized control, is a well-established technique used extensively in power systems ever since synchronous generators were utilized. Since the features between the synchronous generator and the inverter are different, e.g., the inertia of the inverter is low, the traditional droop control needs to be modified in controlling the inverter. In this thesis, to eliminate the traditional droop tradeoff between power sharing and grid voltage, we introduce virtual droop control. In case of transmission impedance mismatch between DG inverter, we use a large virtual resistance in both inverters to match the transmission impedance.

The virtual impedance control is implemented and validated in MATLAB/Simulink and experiment. In this thesis, a microgrid consists of several units are selected for testing.

In conventional droop control, we observe a phase shift between inverter current which cause the circulation current inside the grid. But by using virtual droop control, this circulation current is minimized as well as we obtain a proper power sharing among DG' inverter.

Chapter 1: Introduction

This chapter presents the framework of the thesis which includes various distributed decentralized scheme to get better power quality and power sharing under stable grid condition. This chapter outlines the various renewable technologies, energy storage systems, various type of inverters, and different controlled schema of microgrids.

1. 1 Background

Non-renewable energy sources like natural gas, oil, coal, nuclear reactants begin to deplete in different countries. These conventional energy resources took millions of years inside the earth's core, but most of these resources massively used in different sectors like power generation, transportation, industries in the last hundred years. Because of these reasons, the non-renewable resources will exhaust sooner than anticipated, as we already see this in many countries [1].

Conventional energy sources emit greenhouse gases like carbon dioxide, methane which trapped sun heat in the atmosphere and caused global warming in the last hundred years [1]. Due to excessive heat trapped around the earth, both ocean and land life is highly disrupted. Many seas species face extinction, and we observe the recent fire in the Amazon forest [2], which considers the heart of planet earth. As climate change threatens human existence, the evolving renewable energy in the power system is the only way to mitigate that threat. Stimulated by recent technological developments and increasing concern over the sustainability and environmental consequence of traditional fuel usage, the prospect of producing clean, sustainable power in substantial quantities from renewable energy sources arouses interest worldwide [4].

When electricity generation from renewable technology like the solar plant, wind turbine, the fuel cell connects through the conventional grid is known as a microgrid. Microgrid could operate as both grid-connected mode and self-autonomous islanded mode. As conventional power sources deplete around the world, the self-autonomous microgrid becomes more common. The conventional grid has high inertia, so, when distributed generators from renewable sources operate as grid-connected mode, the turbulence caused by the intermittency nature of DG mitigate by the conventional grid. However, in the islanded mode of microgrid, the power quality is highly disrupted [5].

Electrical power quality effects through different orders of harmonics distortions, low power factor, frequency variation, voltage fluctuation, etc. Nowadays, Power quality has become a concern to electricity consumers on every level; a deteriorated power quality may provide the disappointing response of the electrical equipment and devices and break the power system in numerous ways. Nonlinear loads such as computers, fax machines, printers, PLCs, fridges, Televisions, and electronic lighting ballasts, etc. are one of the major causes of power quality degeneration by the initiation of a switching action and consequently current interruptions. Since exhaustion of conventional electrical power sources set forth the way for renewable energy sources. But without proper control systems, these sources are not compatible with the conventional grids and their integration might add to power quality problems [6].

As the above discussed difficulties, existing grids are under obligation to deliver the increasing demand for power which has suggested the concept of distributed generation systems (DGs) using renewable energy sources (Solar PV, Wind Turbine, etc.) increase production, improves power quality, lowers electricity cost and expenses, which can be accomplished using the approach of smart grids.

A smart grid facilitates the interconnection of different distributed generations known as DGs and regulates the bidirectional power flow between consumer and generating stations [7]. For the implementation of this scheme, a common platform is required for the interconnection of different DGs. This thesis presents a new, efficient, smart, and most importantly a consumer-friendly way of implementing power-sharing in a smart grid, in which the consumer has the freedom of choosing and extracting the proportion of power from DGs available.

1.2 Renewable Energy Technology

With the rapid depletion of the conventional energy sources, an exponential increase in energy demand, and the increasing threat of climate change, energy shift from traditional to renewable energy is inevitable [8]. Moving towards renewable energy will fulfill the target of decreasing greenhouse gas emissions, checking future climate shifts, and ensuring reliable, timely, and cost-efficient energy delivery. For energy security, advances in renewable energy can have significant benefits. Renewable energy sources are continuously renewed by nature and derived directly from the sun (such as thermal and photovoltaic), indirectly from the sun (such as wind, hydropower), or other spontaneous mechanisms and movements of the environment (such as geothermal and tidal power).

This section will outline the renewable energy sources (RESs) like solar PV module, wind turbine and energy storage systems (ESSs). As microgrid system create turbulence under standalone operation or islanded mode these RESs, this paper will discuss the islanded operation of microgrid.

1.2.1 Wind Energy Conversion System

Wind energy is the well-known cost competitive renewable sources. Wind power has attracted much interest in recent years and is currently one of the fastest-growing technologies among all renewable energy solutions [9]. Over 340,000 wind turbines (WT) with a total capacity >591 GW were mounted globally at the end of 2018 [10].

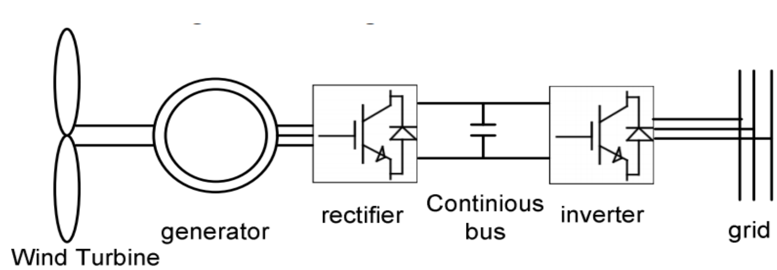

Figure 1.1 : General structure of wind energy conversion system [10]

A general structure of wind turbine energy is shown in figure 1.1, where a wind turbine is connected to a grid using the power converters [11]. Wind turbines transform the kinetic energy of the wind into mechanical power. A generator converts mechanical power into electricity. The mechanical power trapped through the wind turbine is

$$p = \frac{1}{2} \cdot C_p(\lambda, \beta) \cdot \rho \cdot A \cdot v_w^3 \qquad (1.2.1.1)$$

where ρ is the air density, A is the area swept by the blades, v_w is the wind speed, $C_p(\lambda,\beta)$ symbolizes the power coefficient of the wind turbine, β is the wind turbine pitch angle, and λ is the tip-speed ratio (TSR). The wind turbine is characterized by the nondimensional curves of coefficient of performance C_p as a function of tip speed ratio λ. Tip speed ratio h is the ratio of linear speed of the tip of blades to the rotational speed of wind turbine. It can be expressed as follows [12].

$$\lambda = \frac{\omega \cdot R}{v_w} \qquad (2.2.1.2)$$

1.2.2 PV System

Photovoltaic (PV) system is another well-known source of renewable energy which can work in either the standalone mode or grid-connected mode when there is grid. As technology emerges, the grid-connected PV system is getting popular over the time.

Because of intermittent nature of solar radiation, the power generated by PV system fluctuates.

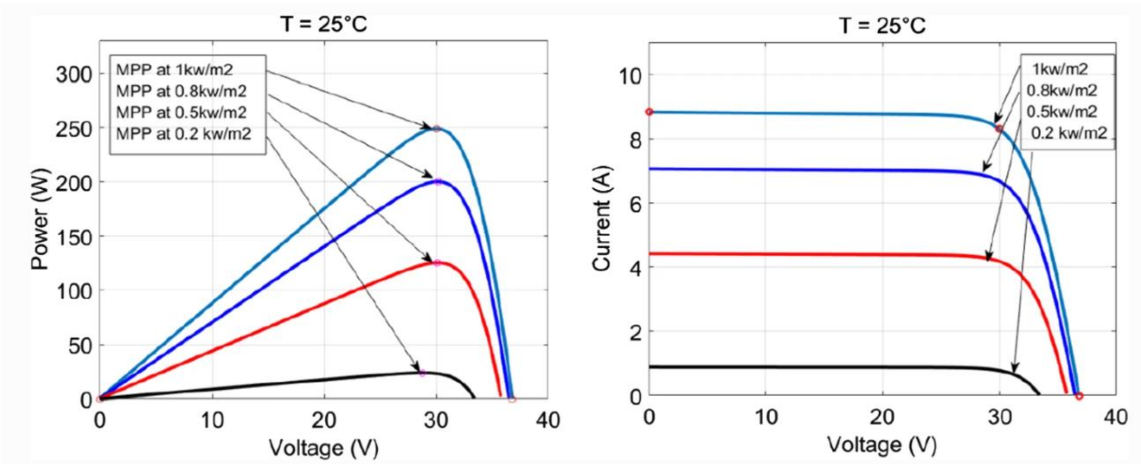

Figure 1.2 : V-P and V-I curve of a solar Module [13]

Figure 1.2 shows the V-I curve for a typical solar panel and output power under different solar radiations. As shown in Figure 2, that the solar power fluctuates with the solar irradiance. For the same solar irradiation, solar power first increases and then decreases with the voltages, therefore, there is only one maximum power point (MPP) under the specific solar irradiation. To extract this MPP, a maximum power point tracker (MPPT) controller is desired to improve solar module efficiency [13].

1.2.3 Energy Storage Systems

Due to intermittence nature of renewable sources, e.g., wind speed and solar irradiances vary with time, installing energy storage systems (ESS) will increase the stability of the voltage, frequency, and power quality. To control voltage and frequency, energy storage devices such as battery and super capacitor are frequently installed in micro grid to increase system inertia to support both load and renewable energy intermittency [10].

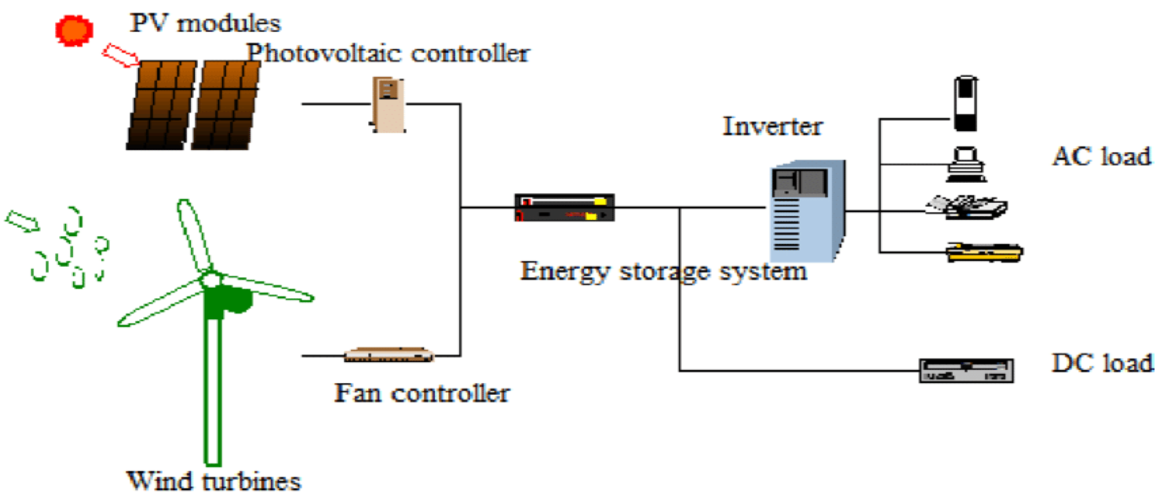

Figure 1.3: Energy storage system in micro grid [10]

In figure 1.3, an ESS is implemented together with PV and wind energy system. Electrical energy system like battery will enhance grid inertia and can be used as a bidirectional with proper charge/discharge controller if system require.

Energy storage systems or ESSs turn out to be an unavoidable part of micro grid. ESS could supply high power density or high energy density in the microgrid, we may choose different storage systems (Like Lead Acid Battery for high energy density, Superconductor for high power density or Lithium ion Battery for both) under different operation of microgrid [10].

1.3 Inverters

As solar PV modules and wind turbines are used in the microgrid system, the inverters from these DGs operate simultaneously. Inverters from different distributed generators need to be synchronized under different line impedances.

In inverter-based DG applications, Voltage source inverter (VSI) and current source inverter (CSI) are the two types of inverter frequently employed. Due to its simple commutation circuit and feedback diodes free operation, the CSI has been used in grid connection applications. However, with the evolution of DG technologies, the VSI design has demonstrated higher efficiency and faster dynamic response, and thus it is more readily controlled to satisfy the conditions of the DG interconnection. In this paper, the VSI is used as the DG interface with the grid [14].

1.3.1 Voltage Source Inverter (VSI)

Through DC/AC inverters, DGs and ESSs connect the microgrid. During the islanded mode, these inverters are usually operated as voltage source inverters (VSIs). These VSIs need to be controlled cooperatively to achieve desired performance and reliability attributes. In AC networks, voltage magnitude and angle difference between connected buses should be regulated in some limited ranges for system security and stability. Frequency synchronization to a nominal value is also essential for grid connection and stability purposes. Besides frequency and voltage regulation, active and reactive power is also considered inherent control objectives in microgrid [14]

DGs, such as PV systems or WTs, are recognized as uncontrollable or non-dispatchable DGs, for their outputs rely on environmental conditions. Conversely, DGs, such as microturbines (MTs) and fuel cells (FCs), are regarded as controllable DGs because they can be controlled smoothly in terms of control signals. In an islanded MG, there is another type of DG. Generally, a battery energy storage system (BESS), called a partially controllable DG, which works in a V/F control mode, and provides the frequency and voltage references for the MG [15].

Controllable DGs operate in PQ control mode, while uncontrollable DGs in maximum power point tracking (MPPT) control mode and the partially controllable in V/F control mode. DGs under the PQ control strategy operate in grid-connected mode, whereas the V/F strategy operates in islanded mode [15]. This section will discuss the PQ control, VF control, MPPT control and coordinate these controls to minimize the fluctuation of frequency, voltage, and power quality on both grid-connected and islanded microgrid mode.

1.3.2 PQ Controlled Inverters

For proper power-sharing in both grid-connected and islanded mode of microgrid, active-reactive power-controlled inverters maintain power ratio defined by the grid operators. In Fig. 1.4, the block diagram of a VSI adopted the PQ control is shown. These control strategies have been used and implemented based on the dq0 reference frame transformation that determines d-and q-axis components of the AC side current. During the simulation, it is assumed that the loads and network's model are shown on the reference frame of one of the individual VSIs [16].

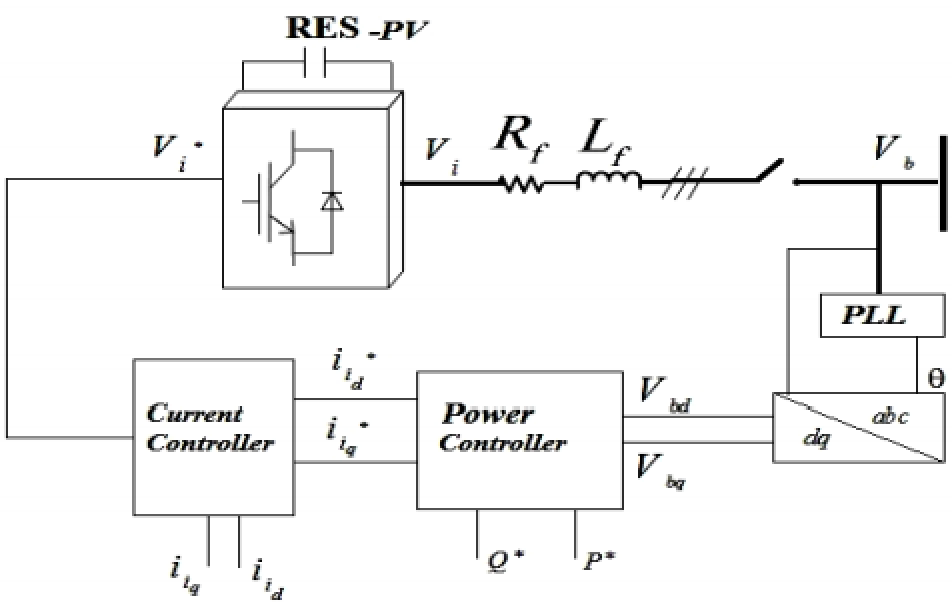

Figure 1.4: PQ Controlled Invertors [16]

1.3.3 Voltage per Frequency (V/f) Controlled Inverters

It is difficult to maintain power quality in the islanded microgrid mode due to the low inertia system. The V/F DG design ensures that its power supply return zero after injecting or absorbing from the grid instantaneously. The DGs will perform voltage and frequency regulation in an autonomous MG operated under VF control (VFDGs). In this case, at least one VSI should be operated in V/F control mode to control the system voltage and frequency within tolerable limits. This control strategy's excellence is that no communication infrastructure is needed, thereby using only local measurements for the MG control in a decentralized method and plug-and-play operation. The block diagram of a VSI adopted V/F control is shown in Figure 1.5. For these units, we will use the conventional droop control strategy.

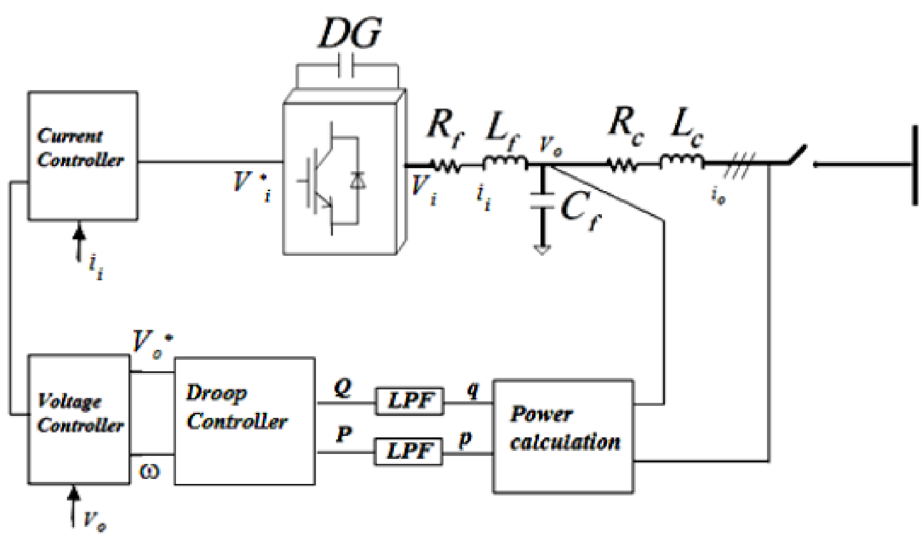

Figure 1.5: V/F Controlled Invertors[16]

1.4 Microgrid Operations

1.4.1 Grid-Connected Control Mode

When the microgrid is operating in grid-connected mode, then the microgrid voltage is maintained by the main grid. The DGs in the microgrid are controlled as power-controlled sources. The VSI acts as a current source in grid-connected (grid-feeding) mode to inject active and reactive power to the grid.

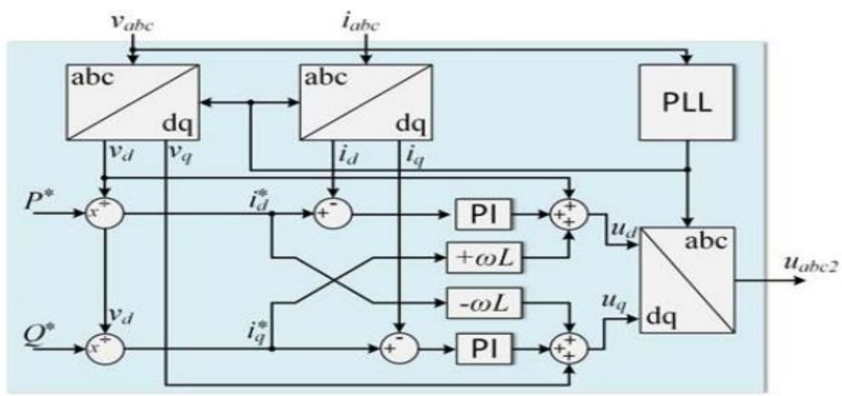

Figure 1.6: Grid Connected Control Mode of Microgrid [17]

In [17], a grid-connected microgrid illustrate using two PQ controlled inverters. In grid-connected mode to supply active and reactive power to the grid, the VSI operates as a current source. A control layout of a grid-connected operation in Figure 1.6 illustrates, which is established on feed-forward-based current control. The reference currents on the dq frame according to [17]

$$i_d^* = \frac{P^*}{v_d} \tag{1.4.1.1}$$

$$i_q^* = \frac{Q^*}{v_d} \tag{1.4.1.2}$$

where P^* and Q^* are the references active and reactive power, sequentially.

1.4.2 Islanded Control Mode

Microgrid islanding may happen in the state of preplanned scheduling or unplanned disruptions. Moreover, the islanded mode has found useful applications in remote or rural areas and geographical islands, where the interconnection with the primary grid is impossible or not feasible.

VSI acts as a voltage source in islanded (grid-forming) mode to generate voltage with a given amplitude and frequency control diagram of islanded operation that is implemented by using cascaded proportional-integral (PI) controllers working on the dq reference frame [17]. A control structure of islanded is shown in figure 1.7, where the external loop controls the inverter output voltage to match its reference value whereas inner loop regulates the current. The output of controller is the set-points of the Space Vector Pulse Width Modulation (SVPWM) for generating the gate signals. The key point in this control structure is that the determination of the reference amplitude and frequency since there are more than one DGs in the microgrid and power sharing between these DGs should be accurate [17].

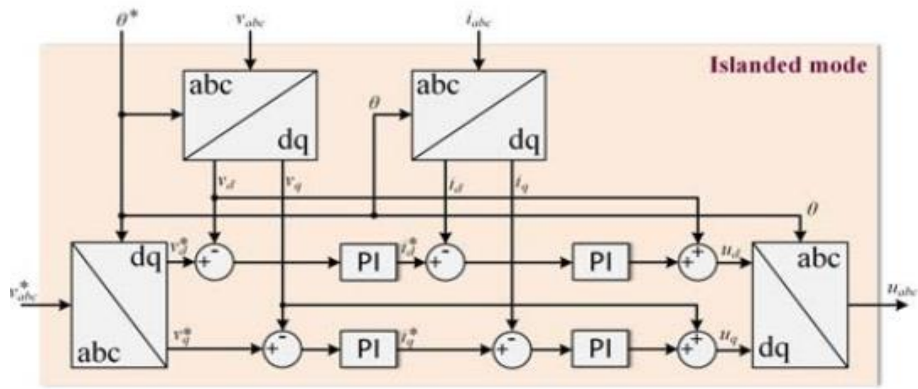

Figure 1.7: Control Structure for Islanded Mode [17]

In the grid-connected microgrid, the system inertia and turbulence created by DGs are mitigated by the connected-grid. As the world transfers from the conventional grid to the microgrid, we would see more islanded microgrid mode. In the Islanded microgrid mode, the system turbulences and power-sharing problems are the main research topics nowadays. This thesis will provide solutions to mitigate voltage, frequency fluctuation after ensuring power quality and proper power-sharing among DGs [17].

1.4.3 Seamless Transfer between Operation Modes

As microgrid will transit from a grid-connected mode to islanded mode, a seamless transition is proposed by [17] in Figure 1.8. According to this proposal, the control structure can separate into three modes: 1) islanded mode control, 2) grid-connected control, 3) seamless transfer between modes.

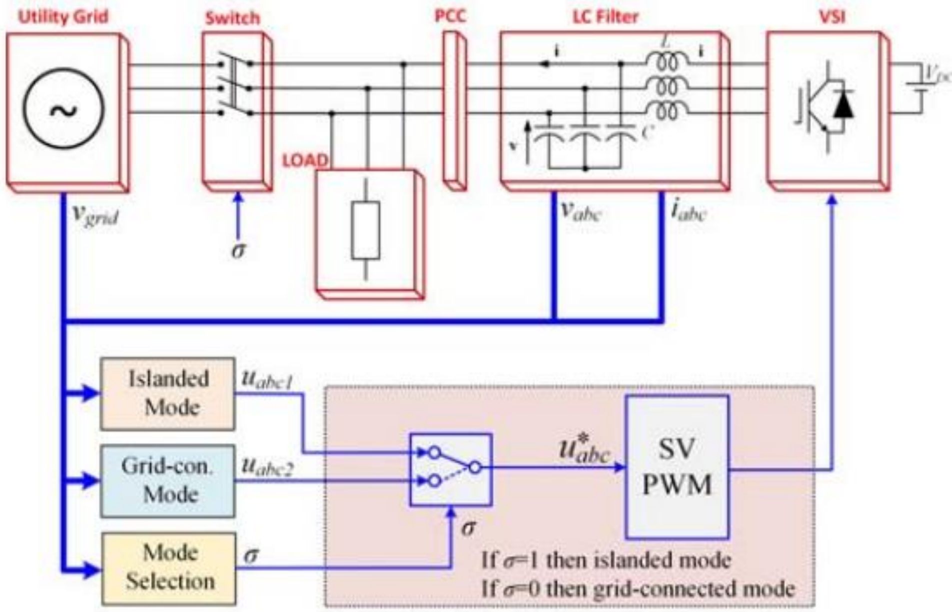

Figure 1.8: Seamless Transfer between Operation Modes [17]

1.5 Phase Locked Loop:

On the network's distribution level, several DGs and a primary grid form microgrid. Due to a continuous variation in demand loads, a wide-range fluctuation in voltage magnitude and frequency occurs at the distribution level. The characteristics of these loads are usually unbalanced and non-linear, which brings harmonics to the system. When the microgrid switch from grid-connected mode to the islanded mode, more variation and transients are caused than grid-connected mode. This research problem adopts the P−f droop control mechanism to share the active power demand during an islanded microgrid. Hence, a ripple-free calculation of the frequency is crucial to generate an active power output constant under steady-state conditions. The PLL employed in a controller algorithm must correctly detect the phase and frequency to maintain stability under severe grid distortion [33].

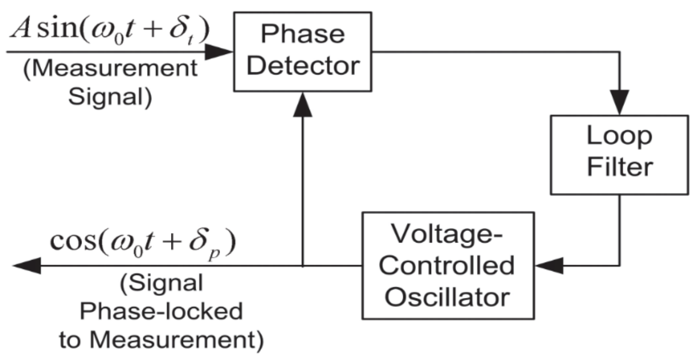

Figure 1.9: Generic PLL block diagram [31]

In Figure 1.9, a block diagram presents the functional elements of a general PLL [31]. The PLL consists of three essential functional segments of a phase detection (PD), a loop filter (LF), and a voltage-controlled oscillator (VCO). The PD measures the phase difference separating the input signal and the output signal and then transfers it to the loop filter for obtaining the DC component. The DC component amplifies and then passes to the VCO, a PI controller, to generate the output signal [32]. The generated frequency integrates to form the phase of the output signal. If the frequency of the output signal synchronizes with the frequency of the input signal, then by using the feedback control mechanism, the difference between the input and the output signal is directed to zero.

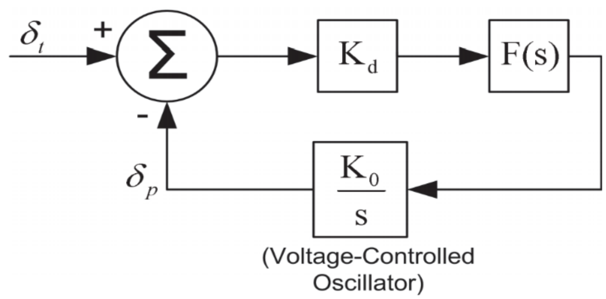

Figure 1.10 : Linearized PLL block diagram [31]

In standard simplifying assumptions, for small variations, allowing the PLL to model according to the linear block diagram of Figure 1.10 where *δt* is the phase of the measured voltage and *δp* is the estimated phase given by the PLL [34].

1.6 Communication topology in a power system

For grid-connected installations, large amounts of generation during low load periods or intermittent generation can lead to difficulty balancing supply and demand, maintaining voltage and frequency stability, and may even result in interruptions due to overvoltage situations tripping protection circuits. In this paper, we present three control methodologies to lessen these difficulties using small-scale distributed battery storage. These three approaches represent three different control architectures: 1) centralized; 2) decentralized; and 3) distributed control.

A. Centralized control: In centralized control, shown in Figure 1.11, one central coordinator receives all the required measurements of the grid, possibly through smart meters and remote terminal units, retrieves the solution to the control problem, and communicates back the set-points to the station. Only in the central control the network component that can initiate a control action [18].

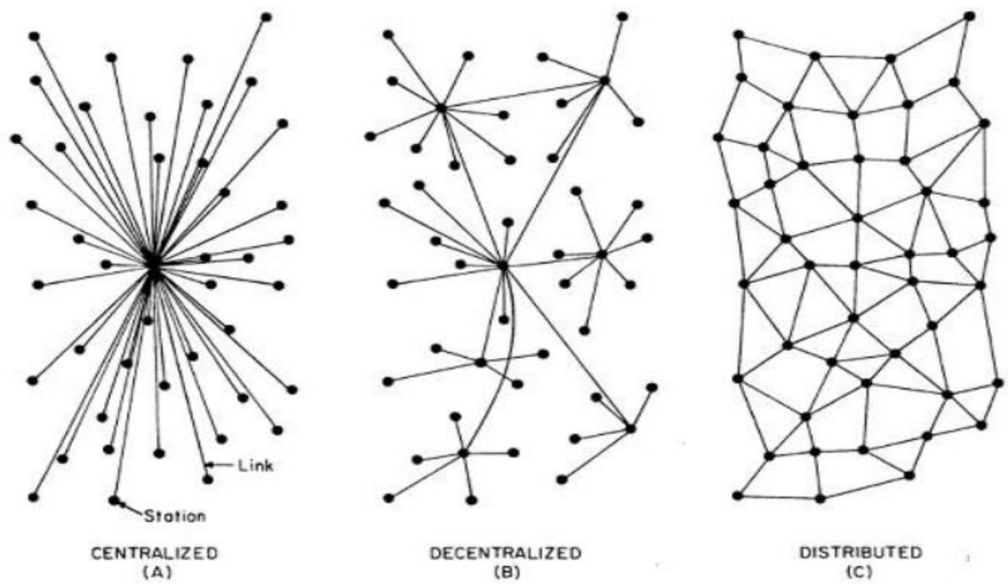

Figure 1.11: Centralized, Decentralized, Distributed Scheme [18]

Since each RES DG must communicate to a central DG, the centralized MPC approach presented above requires a notable amount of communication burden. Additionally, as the network size grows, the computation time required to solve the optimization problem becomes enormous. An additional disadvantage of the centralized MPC approach is that the central entity demands complete information of the network model. Therefore, any change in the network, such as adding new solar resources or batteries, requires the central entity to update its model. As a consequence of these limitations, it is of interest to design decentralized or distributed control approaches that alleviate the communication and computation difficulties, as well as the need for an up-to-date centrally maintained model of the network encountered in centralized MPC [19].

B. Decentralized control: Figure 1.11(B) illustrates an in-between state among centralized and distributed control, which indicates that control is partly centralized and partly distributed regarding the decisions, command/information signals, or computation. A typical case of decentralized control is the network partitioning into zones, where each zone is equipped with its controller (zone coordinator). Each zone functions in the same way as a central coordinator [19].

C Distributed control: each controller needs to communicate only with neighboring nodes, and therefore global knowledge of the grid is not needed to discover the control decision. Intends to reach a self-organized power grid, a distributed coordination structure can cope adequately with the problems that might occur using only local communications and implementing "plug and play" capability [19].

Only distributed and decentralized schemes can offer a robust and flexible control of the distribution network. Moreover, they can deal with limited information and low bandwidth and are much less affected by communication lines errors. All these qualities make them very attractive for smart grid applications [19].

Chapter 2: A Literature Review on Grid Connected Inverters and Research Objectives

This chapter will evaluate the different communication networks in an islanded microgrid, microgrid control parameters, and grid components like PLL. This chapter will discuss the voltage and frequency regulations, power quality, and how these microgrid parameters are determined.

2.1 Communication Network in Microgrid

Communication-based control techniques such as distributed, decentralized can achieve excellent voltage regulation and power-sharing in the microgrids. Compared to droop controllers, the output voltage amplitude and frequency in these control techniques are generally close to their reference values [20]. However, these control strategies require communication lines between the modules, resulting in increased system cost. Long-distance communication lines will be easier to get interfered, which reduce system reliability and expandability [20]. In the following section, several typical communication-based control strategies in microgrid operations are reviewed.

The microgrid control system based on communication network could be classified into three categories: centralized control, distributed control, and decentralized or master-slave control [9].

In local control, DGs have no communication and IEDs or intelligent electronic devices in local control schema, only measure the point of standard coupling voltage and frequency.

In centralized control of microgrid, one central coordinator receives all the information from connected DGs through the communication channel, as shown in Figure 2.1. In the case of parallel units controlled by synchronization signals, they have negligible differences of frequency and phase among each other; thus, the current sharing error of each unit can be caused by voltage amplitude inaccuracies. Therefore, this method directly adds current error to each inverter unit as a compensation component of the voltage reference to eliminate the differences among their output currents [9].

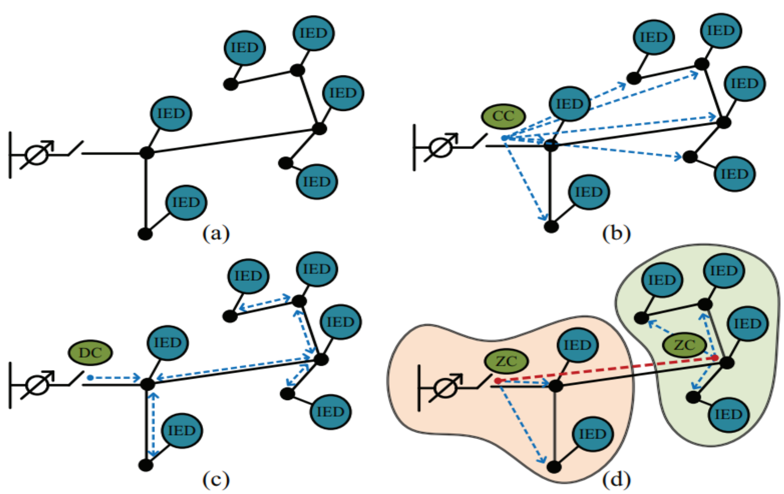

Figure 2.1: Classification of control schemes based on their communication network: a) local control; b) centralized control; c) distributed control; and d) decentralized master-slave control [9]

One advantage of the concentrated method is that current sharing can be maintained during both steady-state and transients. However, this control scheme must include a centralized controller, making it challenging to expand the system and reduce system redundancies [21]. Moreover, current reference must be distributed to all converters using high-bandwidth communication links to achieve synchronization among the units. These techniques present high dependency on communications and reduce the reliability, which may be compromised with single-point faults [21].

In distributed control, a distributed coordinator or grid operator interfaces with other DGs is shown in Figure 2.1. In this scheme, all IED corporate with the neighbor node to reach a typical control arrangement set by the grid operator, and hence global information of the grid (i.e., the state of all nodes) is not required in order to determine the control decision [9]. The decentralized control introduces a control scheme that is partly centralized and partly distributed concerning the arrangements, command/information signals, or computation. In decentralized control, the system is partitioning into the zones, where each zone is provided with its controller that operates identically as a central coordinator in its region and these controllers might be loosely linked for coordination purposes, in similarity with distributed control, to accomplish a distinct purpose [9].

Both distributed and decentralize control schemes are robust compare to other control systems. In this thesis, only distributed control scheme will be simulated and validated in the experiment with a proper control system.

This thesis chooses distributed communication because low bandwidth is required, e.g., only the nearest neighbor information is required.

2.1.1 Impact of Communication Delay and data loss in a microgrid

Although most of the microgrid research papers discuss the external cyber-security issue, ignore the inherent time delay or data loss during the communication channel's data transmission [22], however, few papers [23]-[24] analyzed the consequence of the data error and loss on the demand response control system. They showed that the control error would be intolerable if the data error ratio is more than 4%. Besides the data error, the inherent time delay is another factor that can affect the power system operation. References [25]-[26] investigated the time delay margins of the islanded microgrid control and the multi-grid coordinated control, respectively. They conclude that if the time delay exceeds the tolerable margins, the microgrid operation will be unstable.

For the Synchronization part, the dedicated low-latency communication system is necessary because the time delay should be lower than 1μs; otherwise, the carriers whose frequencies are usually dozens of kHz cannot be well synchronized [27].

2.2 Distributed Generation

Electricity generated from renewable sources refers to distributed generation, and these sustainable resources when producing electric power denotes as a distributed generator. DG could be described as electric power generation within distribution grids on the network's customer side. According to the Electric Power Research Institute, DG's size ranges from a few kilowatts to 50 MW [32].

Grid-connected distributed generators' operational characteristics differ slightly from conventional power generators. Grid-connected conventional power generators are synchronous generator and high inertia; therefore, they would provide the necessary reactive power to the grid when required. However, islanded distributed generators are asynchronous generator (also known as induction generator) and low inertia; therefore, would not supply the reactive power to the grid unless it is connected to the conventional generators or connected to high inertia associated VF controlled DG as discussed before [30].

A group of the islanded asynchronous generators is not capable of producing reactive power without the power electronics or control method [30]. In grid-connected mode, asynchronous generator demands reactive power from the grid during the start-up process and at operation. Various technical alternatives exist to overcome the limitations of grid-connected asynchronous generators. Micro-grid specialists suggest a wide range of options for operational distributed generators, such as the battery, fuel cells, supercapacitors, and power electronic converters [30].

The control schemes for the applied microgrid can be classified based on communication or exchanging the information between entities. We prefer the distributed scheme over other control systems because of this control's robustness and minimum communication between entities.

2.3 Classifications of Distributed Generators based on controllability

The voltage source inverters of DGs can be operated in Active-Reactive Power Control Mode (PQ Mode) and Voltage-Frequency Control Mode (VF Mode). We might coordinate or exchange information between these inverters' mode under different conditions (grid-connected and islanded mode). Moreover, coordination between different inverters is challenging [16], [28].

Distributed generators from various sources such as photovoltaic, wind turbine, fuel cell, and energy storage system may integrate into MGs under different circumstances, and the interaction between the power grid and distributed generators (DGs) are complicated.

DERs are considered as Uncontrollable or non-dispatchable as energy extraction depends on the environment in these sources. These uncontrollable DG operate as the MPPT Mode of voltage source inverters. The DGs are generated from a fuel cell, and microturbine is known as controllable or dispatchable because the amount of power can be controlled. These types of DGs work as a PQ control of VSIs. In islanded mode, there is another type of DG, in which energy storage system is integrated known as partially controllable DG, which works in a V/F control mode and is responsible for regulating voltage and frequency in islanded mode [16], [28].

2.4 Frequency and Voltage Regulation Constraints

While the large-scale deployment of a microgrid is composed of intermittent sources (wind, solar) with uncertainty, Frequency and voltage regulation are two of the most important factors.

Unlike a centralized control, a decentralized control schemes transform frequency and voltage regulation into a local task in DGs. In the decentralized scheme, the information share among neighboring units; thus, the microgrid performance is affected by the grid network scheme [35].

According to the ANSI/NEMA C84.1 standard, the standard frequency variation should be within ±0.5 Hz, and the voltage must be kept in between 0.9 p.u to 1.1p.u. [37].

In terms of voltage-frequency control, there are significant distinctions between microgrids and conventional power grids. In traditional power grids, the voltage regulation is performed widely by large synchronous generators implemented with Automatic Voltage Regulator (AVR) [35] or by other equipment such as power transformer tap changers. Automatic Generation Control (AGC) regulates the traditional power system frequency, which manages large synchronous generators equipped with the governor. In the grid-connected mode, voltage and frequency regulation are relatively fixed because of the system's voltage and frequency control by the primary grid [36] . In this mode, each DG injects current to the microgrid, which can be taken as a current source. Therefore, these

DGs operate in the active-reactive power control mode (PQ mode). However, in the islanded mode, the voltage and frequency are mainly regulated through inverters or DGs converters. Thus, some inverters/converters of DG units are operated in the voltage-frequency (VF) control mode to control voltage and frequency, others can be operated at PQ mode to inject active/reactive power to the microgrid. Since microgrids face more challenges in the islanded mode than the grid-connected mode, we focus on microgrids' performance in the islanded mode. Microgrids need to control voltage and frequency after variation in demand power, generations, and communication topology [37].

Studies have presented two control loops for voltage and frequency regulation of inverters in self-sufficient microgrid [36]. In these control structures, the first control loop is mainly the power control loop, where the droop characteristic of synchronous generators is used to keep frequency and voltage at their nominal values. The P and Q values obtained from the power measurement block are feeds to the voltage control block to eliminate the voltage error. Voltage controllers such as the proportional-integral (PI) regulator can eliminate voltage error. Later the voltage controller's output feeds to the current controller block as the last control unit. In control structures, both voltage and current controllers are placed usually in a back to back situation. Eventually, the signal gained from the current's controller block generates drive signals for the VSIs using the space vector PWM module [37].

2.5 Research Objectives

The main research object of this thesis is to develop and validate the model of inverters' grid synchronization. DGs can be operated in both PQ and VF mode. PQ controlled distributed generators will provide power sharing and VF controlled DG will provide the stability of grid frequency and voltage.

Proper Active-Reactive Power Sharing: As multiple distributed generators operate simultaneously, active-reactive power sharing is important to power management of the microgrid. In grid-connected mode, conventional grid may supply all the system demand power. But in islanded mode, maintaining proper power sharing ratio could be difficult because of divergence of demand power might not abated by conventional grid. In such case, the electric storage system will minimize the system turbulence created by both deviation of demand power and intermittency of DGs. This thesis will specifically address the active-reactive power sharing in islanded mode of micro-grid.

Steady Grid Voltage: The grid voltage or point of common coupling voltage (also known as V_{PCC}) need to be kept steady. This common voltage is in low range compare to primary grid generation voltage and highly differs as both connected load and power supply from renewable sources fluctuates with time.

Stable Grid Frequency: Even though the inverter might produce stable grid frequency if storage system is installed to provide the inertia, but grid frequency might vary with load fluctuation. When the load power is more than system power, the grid frequency will fall slightly and vice versa. It's important to supply stable grid frequency for AC load system.

Chapter 3. Different Control Strategies of Microgrid

In microgrid (MG) islanded operations, it is not common to find fully controllable synchronous generators generally for voltage and frequency control in conventional power systems. Due to the intermittent characteristics of renewable sources, most distributed generators installed in an MG are not suitable for connecting to the electrical grid directly. For example, induction/asynchronous generator operated WT is not capable of controlling voltage or reactive power. Therefore, power electronic interfaces (DC/AC in PV or AC/DC/AC in WT) are required. Inverters control and coordination is thus the fundamental concern in MG [38].

3.1 Conventional Droop Control

To meet the expanding electricity demand, coordination of different distributed generation (DG) units is essential. Various control strategies, such as droop control, master-slave control, and average current-sharing control, have been widely performed worldwide to operate parallel-connected inverters for load distribution in the DG network. Communication-based control strategies deployed to interact between the DG inverters. However, too many communications signals lead to a complex structure of the microgrid and inhibit expansion. Among these methods, the droop control technique (control strategy based on active and reactive power) has been widely used because of the absence of communication among parallel-connected inverters to coordinate the DG units within a microgrid. Droop control mitigates the microgrid problems such as reverse droop control, hierarchical droop control, improved droop control, and virtual power droop control [39]. This chapter will discuss a few of these controls.

3.1.1 Power Flow Analysis in Droop Control

Two parallel inverters are analyzed to illustrate the power flow analysis and operational principle of droop control in this subsection. As the synchronous generator, an inverter can also be modeled as a voltage source in series with an internal impedance [39] in islanded mode. The model of two parallel-operated inverters is shown in Figure 3.1.

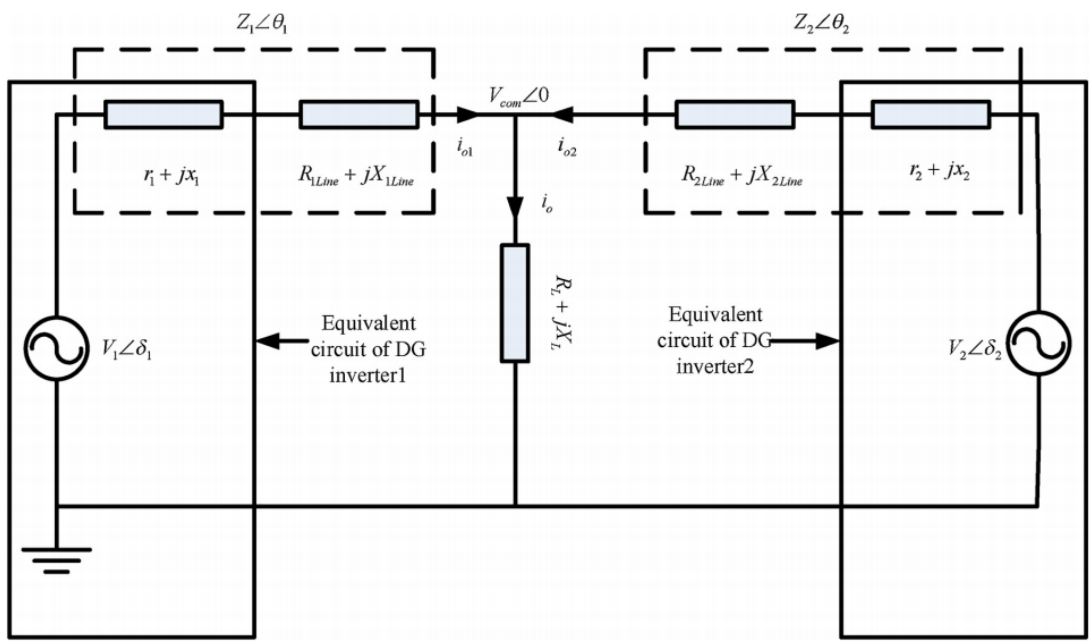

Figure 3.1 : DG Inverters equivalent circuit in autonomous mode [39]

A simplified schematic of parallel DG inverters is shown in Figure 3.1. The total impedance of the DG 1 is the sum of equivalent circuit output impedance and the line impedance.

$$Z_1 = r_1 + jx_1 + R_{1L} + jX_{1L} = Z_1\angle\theta_1 \quad (3.1.1)$$

The sum of output impedance and the line impedance of the DG 2 is given by

$$Z_2 = r_2 + jx_2 + R_{2L} + jX_{2L} = Z_2\angle\theta_2 \quad (3.1.2)$$

where r_1, r_2 are the inverters output resistances; x_1, x_2 are the inverter equivalent output reactance; R_{1L}, R_{2L} are the line resistances; X_{1L}, X_{2L} are the line reactance; $V_{PCC}\angle 0$ is the point of common coupling AC bus voltage; V_1, V_2 are DG inverter output voltages; δ_1, δ_2 are the DG inverter output voltage phase angles; θ_1, θ_2 are the total impedance angles of DG inverters; i_{o1}, i_{o2} are the output currents of DG inverters; and i_o is the load current [40].

The DG inverters output current and power is given by:

$$i_i = \frac{V_i\angle\delta_i - V_{PCC}\angle 0}{Z_i\angle\theta_i} \quad (3.1.3)$$

$$S_i = V_i\angle\delta_i \times i_i^* = P_i + jQ_i \; (i = 1,2 \ldots .n) \quad (3.1.4)$$

where n is the number of DG inverters; P_i and Q_i are the active and reactive power output of the i^{th} DG inverter respectively which are expressed as:

$$P_i = \frac{1}{Z_i}[(V_i V_{PCC} cos\delta_i - V_{PCC}^2)cos\theta_i + V_i V_{PCC} sin\delta_i sin\theta_i] \tag{3.1.5}$$

$$Q_i = \frac{1}{Z_i}[(V_i V_{PCC} cos\delta_i - V_{PCC}^2)sin\theta_i - V_i V_{PCC} sin\delta_i cos\theta_i] \tag{3.1.6}$$

When the sum of output impedance and line impedance is purely inductive, i.e., $\theta_i = 90^0$, then the Equations (3.1.5) and (3.1.6) can be simplified as:

$$P_i = \frac{V_i V_{PCC}}{X_{iL}} \delta_i \tag{3.1.7}$$

$$Q_i = \frac{V_i V_{PCC} - V_{PCC}^2}{X_{iL}} \tag{3.1.8}$$

From equations (3.1.7) and (3.1.8), the power angle δ_i determines the flow of active power, whereas voltage amplitude V_{pcc} determines the flow of reactive power. The active power is proportional to phase angle δ_i.

3.1.2 P-f/Q-V Droop Control for Inductive Transmission Line

For inductive transmission lines or X-dominated lines, the P-f/Q-V droop control strategy can be used as illustrated in Figure 3.2

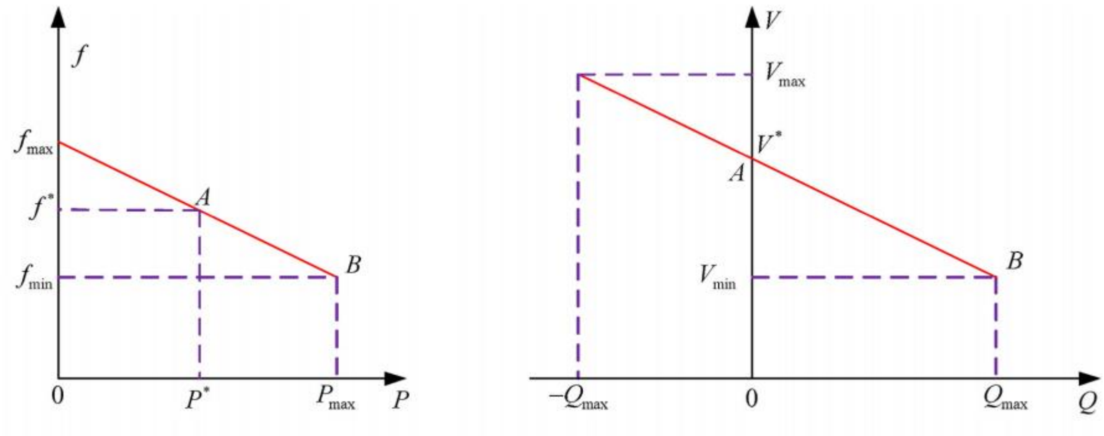

Figure 3.2: P-f/Q-V droop control curve [39]

The P-f/Q-V droop control curve is shown in Figure 3.2 and control equations are given by [40]

$$f_i = f_i^* - m_i(P_i - P_i^*) \tag{3.1.9}$$

$$V_i = V_i^* - n_i(Q_i - Q_i^*) \tag{3.1.10}$$

where $f_i^*$and V_i^* are the voltage amplitude and frequency of the DG inverters; m_i , n_i are the P-f/Q-V control coefficients; P_i^* and Q_i^* are respectively the rated active and reactive power of the i[th] DG inverter output. The value of m_i and n_i for P-f/Q-V could be defined as

$$m_i = \frac{\Delta f}{P_{max}}, n_i = \frac{\Delta V}{Q_{max}}$$

3.1.3 P-V/Q-f Droop Control for Resistive Transmission Line

In low-voltage (LV) microgrids, active power/voltage (P/V) droop controllers are increasing attention as they take the network lines' resistive nature and the lack of directly joined rotating inertia into account. There is a relationship between P and V in resistive networks, such that P-V/Q-f droop controllers are useful.

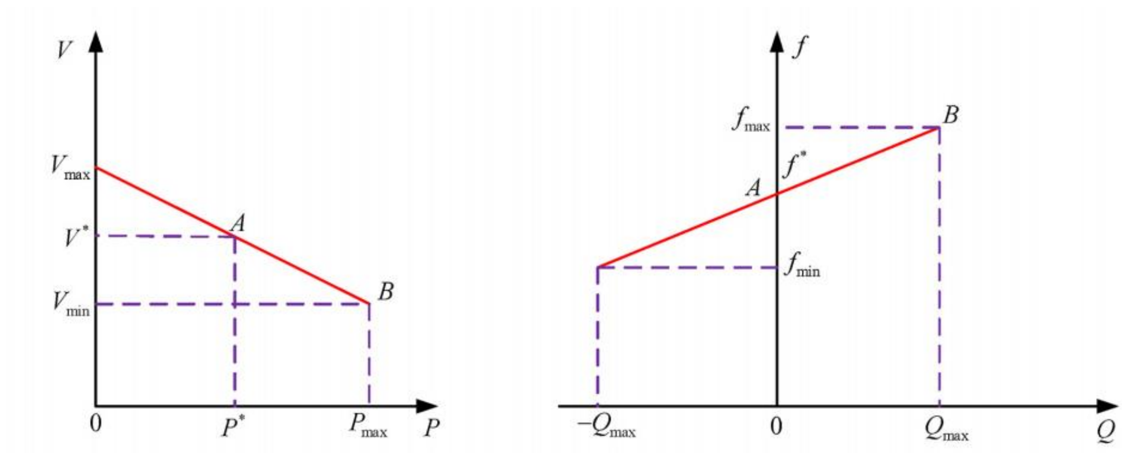

Figure 3.3 : P-f/Q-V droop control curve [39]

The P-V/Q-f droop control curve is shown in Figure 3.3 and control equations are given by

$$V_i = V_i^* - m_i(P_i - P_i^*) \tag{3.1.11}$$

$$f_i = f_i^* + n_i(Q_i - Q_i^*) \tag{3.1.12}$$

$$m_i = \frac{\Delta V}{P_{max}}, n_i = \frac{\Delta f}{Q_{max}}$$

3.1.4 Power distribution condition between DG inverters

When the parallel DG inverters are operated in an isolated mode, each DG inverter's output frequency and V_{PCC} should be properly controlled to minimize the circulation current or stable grid [40]-[41]. The droop control method to achieve a reasonable distribution of the load power needs to meet the following equations for inverter A and B.

$$m_A P_A^* = m_B P_B^*\,, \qquad n_A Q_A^* = n_B Q_B^*, \qquad f_A^* = f_B^*\,, \qquad V_A^* = V_B^* \tag{3.1.13}$$

$$\delta_A = \delta_B\,, \qquad \frac{X_{AL}}{m_A} = \frac{X_{BL}}{m_B}, \qquad V_A = V_B, \qquad \frac{X_{AL}}{n_A} = \frac{X_{BL}}{n_B} \tag{3.1.14}$$

$$n_A P_A^* = n_B P_B^*\,, \qquad m_A Q_A^* = m_B Q_B^*, \qquad f_A^* = f_B^*\,, \qquad V_A^* = V_B^* \tag{3.1.15}$$

$$\delta_A = \delta_B\,, \qquad \frac{R_{AL}}{m_A} = \frac{R_{BL}}{m_B}, \qquad V_A = V_B, \qquad \frac{R_{AL}}{n_A} = \frac{R_{BL}}{n_B} \tag{3.1.16}$$

Equations (3.1.13)– (3.1.16) reveal that to ensure the proportional sharing of active and reactive power of parallel DG inverters A & B, it is crucial to satisfy the following requirements: 1) DG inverters A& B voltage and frequency should match the rated value; 2) Inverter droop coefficients should be inversely proportional to the rated capacity; 3) The line impedance at the output of each DG inverter is inversely proportional to droop coefficients; 4) The output voltage of each DG inverter should have equal amplitude and phase.

Increasing the droop coefficients results in good power-sharing but degraded voltage regulation. The inherent trade-off between power-sharing and voltage regulation of this controller is selecting the droop coefficient m_i, n_i value [42]. The droop control technique's benefit is there is no communication requirement among parallel-connected inverters, which provides significant adaptability [42]. However, the conventional droop technique has numerous shortcomings [43]-[44], e.g., slow transient response, an inherent trade-off between voltage regulation and load sharing, poor harmonic load sharing between parallel-connected inverters in the case of non-linear loads, the line impedance mismatch among parallel-connected inverters that affect active and reactive power-sharing, and poor performance with renewable energy resources.

The output impedance of the inverter and line impedance to the load is different, considering the geographical location and other factors, with a certain degree of randomness, it is challenging to satisfy equations (3.1.13)– (3.1.16) and is challenging to realize the proportional power-sharing between the DG inverters according to the P-f/Q-V, P-V/Q-f droop control schemes [39]- [41].

3.2 Virtual Impedance Droop Control

When distributed generation inverters are generally operated parallel with conventional P-f/Q-V, or P-V/Q-f droop control approaches, due to mismatched resistive and inductive line impedance, the parallel DG inverters' power-sharing and output voltage diverge from the reference value, which leads to instability in the microgrid system. Adding virtual resistors and virtual inductors in the control loop of droop controllers improve reactive power-sharing and stability. However, this leads to a voltage drop [42].

Under the line impedance mismatch, the conventional droop control cannot balance reactive power-sharing among parallel-connected inverters. Consequently, the imbalance in reactive power-sharing is a severe problem in an AC microgrid. Several studies have achieved balanced reactive power sharing implementing virtual output impedance in the droop control method through a fast control loop that emulates the line impedance [45]-[46]. Thus, the reference voltage from each inverter can be adjusted, as follows:

$$V_{ref} = V_o^* - Z_v I_o \tag{3.2.1}$$

where Z_v is the virtual output impedance which is generally selected to dominate line impedance and modified inductive or resistive transmission virtual impedance will allow P-f or P-V droop control [47]. Thus, the virtual output impedance can be chosen through the summation approach, in which balanced reactive power sharing is achieved if the voltage drop from every inverter to AC bus is as follows [48]:

$$V_{droop1} = (Z_{l1} + Z_{v1})I_{l1} = V_{droop2} = (Z_{l2} + Z_{v2})I_{l2} \tag{3.2.2}$$

Hence, Z_{v1} and Z_{v2} are the virtual output impedance of two parallel connected inverters. Furthermore, Z_{l1} and Z_{l2} are line impedance of two parallel connected inverters, respectively.

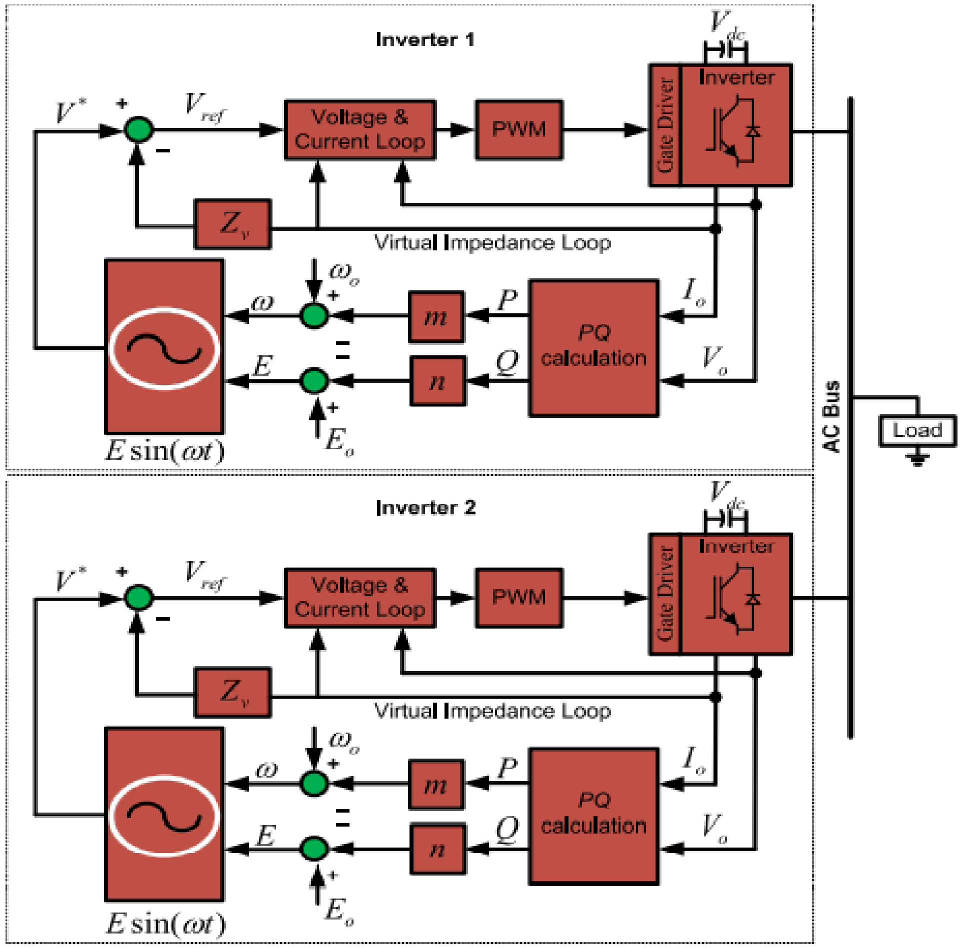

Figure 3.4: Virtual impedance loop-based droop control [42]

If we set the virtual output impedance of DG is zero, and we can emulate the other DG' virtual output impedance. Based on Eq. (3.2.2) and considering that one line impedance is larger than others, that is , $Z_{l1} > Z_{l2}$ which permits the selection of Z_{v1}= 0, and Eq. (3.2.2) can be simplified as follows:

$$Z_{v2} = Z_{l1} - Z_{l2} \tag{3.2.3}$$

Using the summation approach, the value of the virtual impedance is decreased, which reduces the degradation of voltage regulation. Reactive power-sharing is improved if the output voltage change is markedly more significant than the voltage drops across the line than the reactive power. In this thesis, we will use a large virtual resistance to maintain reactive power-sharing.

3.3 Agent-based communication framework

An agent performs as a local control processor and communication devices, so agents can collect present states of distributed generators (DGs) and loads when communication lines are added between two layers. Furthermore, each agent can also transfer information with its adjacent agents of the microgrid islanded network. After the information is processed according to control laws, agents regulate DGs' production to which they connect [49].

Multiagent system (MAS)-based methods have emerged in decentralized control, optimization, and energy management for MGs. In [50], a decentralized MAS-based frequency control strategy was investigated for an islanded MG, when agents were only allowed to exchange information locally. A distributed control approach was also studied when the system consists of more than one MG agent or multi-MG agents.

3.4 Two Layer Control Model for Microgrid

In the distributed scheme of the microgrid could be operated as two layers. The top layer is the communication network over a microgrid as the bottom layer. A systematic method is applied to derive a set of distributed control laws for agents from any given communication network, where only the nearest neighbor information is needed [52].

3.5 Dynamic Weights control of distributed inverters

The control laws consist of two terms: 1) dynamic and 2) fixed weights, in which the term with dynamic weights reassigns outputs of distributed generators to reach different targets [51].

The gradient descent due to voltage and frequency fluctuation in the microgrid's islanded mode is measured in VF controlled distributed generators. Instantaneous active, reactive power gradient is measured in VF controlled DG. Furthermore, this decent gradient power is appropriately scaled between other PQ and MPPT controlled DGs to maintain power quality with proper inertia and unscathed in high system turbulence due to sporadic demand power. This method offers a convenient way to achieve different control and management targets by substituting a parameter in the control laws with dynamic weights. More importantly, the control laws with dynamic weights never break the system balance during iterations.

Chapter 4. Investigating several microgrid control models

In this thesis, we examine both grid-connected and islanded microgrid. As discussed before, in chapter one, in the grid-connected mode, the primary grid has sufficiently large inertia to mitigate system turbulences caused by both the intermittent nature of renewable DG and demand power. And we will also be able to get the power-sharing under stable grid frequency and voltage.

This chapter will simulate several control strategies of the microgrid, which discuss in the previous chapter. First, it will examine the grid-connected microgrid mode using two PQ controlled DGs and one primary grid generator. It would simulate under different transmission line impedances and various power-sharing between DGs. In different transmission impedances, how the PI controller gains change and will draw a relation between these.

Then, we will simulate the microgrid in the island mode. As discussed in the chapter one, the island microgrid situation will increase day-by-day as we see a transition from conventional power to renewable power. At the beginning of the islanded microgrid, we implement the virtual impedance droop control strategy and discuss simulation findings and limitations under different conditions.

To overcome the limitation of large resistance virtual impedance droop control strategy, finally, we will propose a decentralized multiagent-based communication using V/F controlled DG. We will implement a secondary hierarchical droop control in V/F DG to overcome the dynamic power-sharing.

In a grid-connected mode of the microgrid, the V/F control DG will work as a PQ-controlled DG. But when the grid senses an islanded grid, it will switch to V/F controlled immediately.

4.1 Grid Connected Mode of Microgrid

When distributed generators connect to the conventional grid is known as the grid-connected mode of the microgrid. In grid-connected mode, the DG inverter operates as a current source inverter. In this simulation, two PQ control distributed generators and one conventional grid connect in the microgrid.

Simulation Setup

We have applied two PQ controlled DGs as converter 2 and 3, where two PI controller controls active and reactive power by changing the continuous reference voltage and phase angle. Converter 1 is considered a conventional grid that will provide the additional inertia to the system to get the power sharing and grid stability (Grid frequency, Voltage). In each converter, we apply different transmission line impedances to illustrate the practical set-up in the grid.

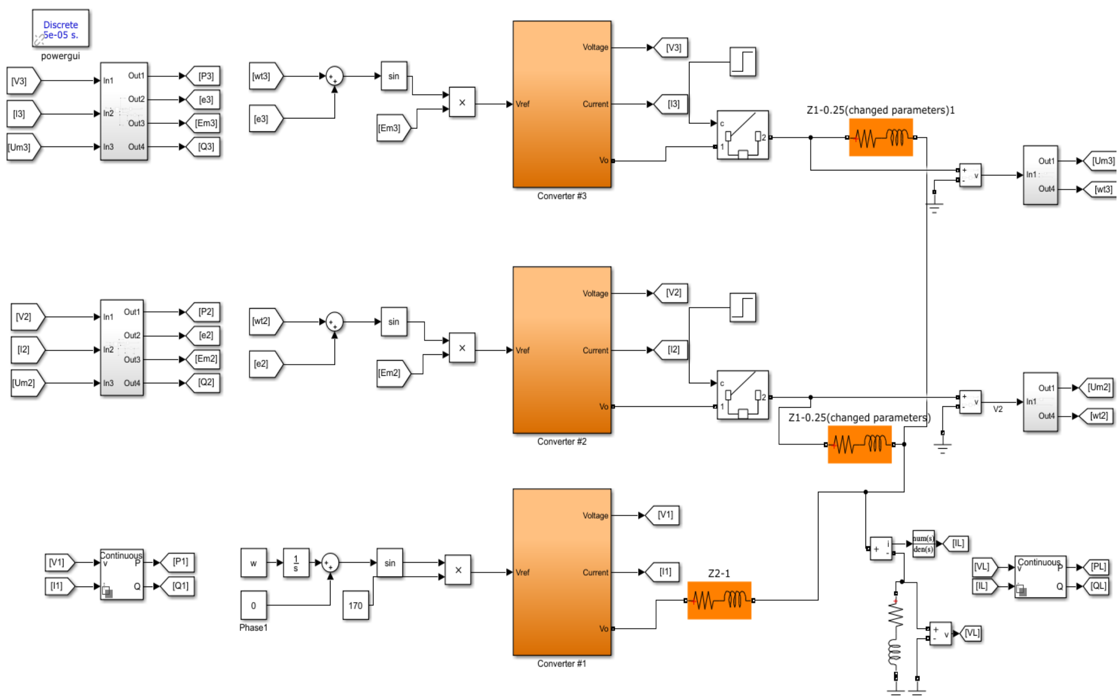

Figure 4.1: Grid Connected MATLAB/Simulink Model

Simulation Parameters are listed in Table 4.1

Table 4.1 Grid Connected MATLAB/Simulink Model Parameters

Parameters	Value	Unit
Grid Frequency	Hz	60

Grid Voltage Peak Value	Volt	170
Grid Transmission Resistance	0.1	Ohms
Grid Transmission Inductance	3e-6	H
DG2 Transmission Resistance	0.05	Ohms
DG2 Transmission Inductance	1.5e-6	H
DG3 Transmission Resistance	0.15	Ohms
DG3 Transmission Inductance	4.5e-6	H
DG3 Active Power Kp	1.1131e-07	
DG3 Active Power Ki	159.8	
DG3 Active Power Gain	10	
DG3 Reactive Power Kp	9.0544e-06	
DG3 Reactive Power Ki	479.9	
DG3 Reactive Power Gain	200	
DG2 Active Power Kp	5.4e-9	
DG2 Active Power Ki	3881	
DG2 Active Power Gain	10	
DG2 Reactive Power Kp	4.3754e-07	
DG2 Reactive Power Ki	4342	
DG2 Reactive Power Gain	200	
Connected Reactive Power	300	Watt

Connected Active Load	1200	Watt

Simulation Outputs

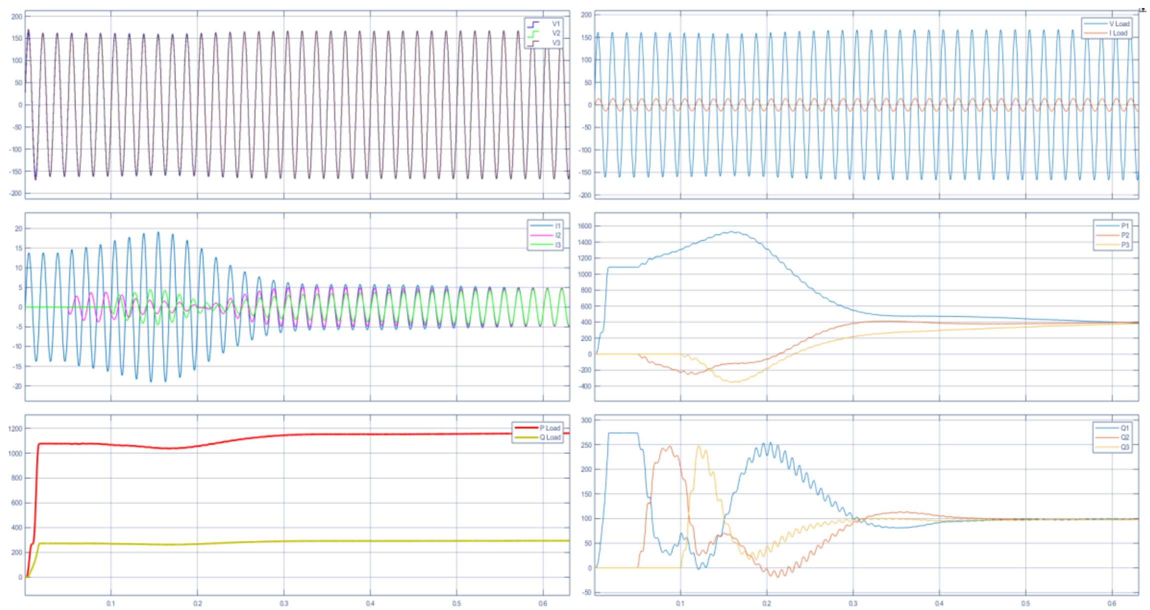

Figure 4.2: Grid-connected Simulation output

Both active and reactive power sharing obtained based on the power reference in PQ-controlled DGs. We choose the proper PI controller parameter to do that. In the case of impedance mismatch between DG1 and DG2, we have to apply the same gain ratio to have equal power-sharing..

We have found stable frequency and power-sharing after 0.4s in Figure 4.2 and improved the initial turbulence after adjusting DG switching in the grid.

4.2 Islanded Mode of Microgrid

As chapter 3 discusses, using conventional droop control (P-f/Q-V and P-V/Q-f) according to transmission line impedances for power-sharing, we have to trade-off between the point of common coupling voltage (Vpcc) and power-sharing. Moreover, the reactive power-sharing cannot control using this droop control when the transmission line impedance mismatch between DGs.

We try to implement large resistance virtual impedance P-V/Q-f droop control to eliminate the disrupted reactive power-sharing. By using large virtual resistance, the line impendence tends to be close.

4.2.1 Virtual Resistance Droop Control

In this setup, we discarded the conventional inverter from the previous simulation to create the islanded mode.

In microgrid control mode, both PQ-controlled DGs work alone to have a stable grid and power-sharing intermittent nature of distributed generators and demand power. As chapter 3 discusses, we have applied the large resistance virtual droop control between these DGs. To maintain accurate power-sharing without distorting grid voltage,

we added large resistance in the intention of using P-V/Q-f droop control.

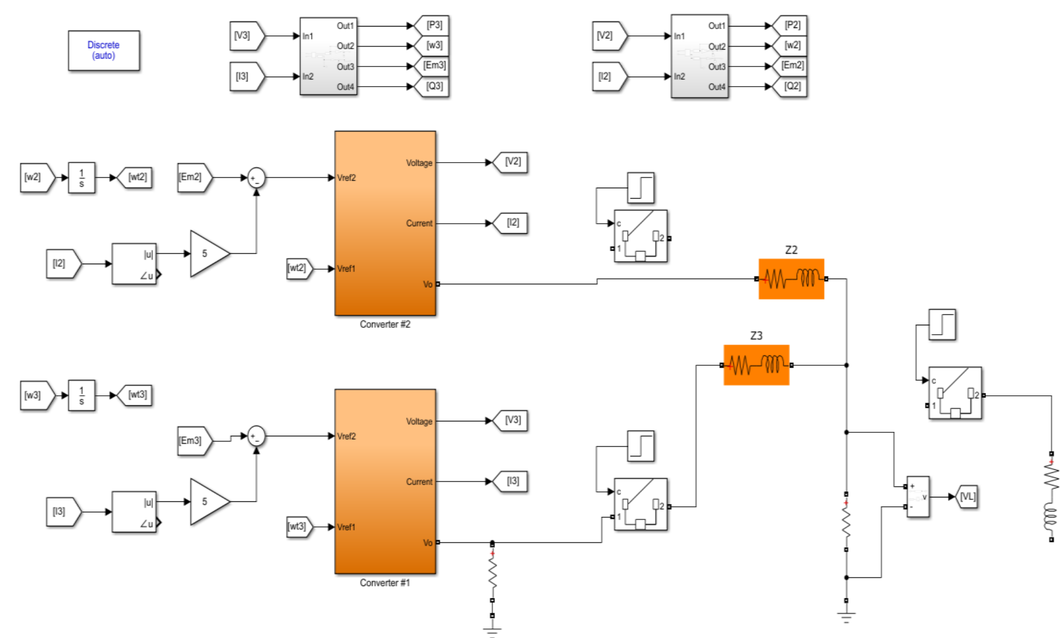

Figure 4.3: Large Virtual Resistance MATLAB/Simulink Model

Simulation Parameters are listed in Table 4.2 for simulation Figure 4.3

Table 4.2: Large Virtual Resistance MATLAB/Simulink Model Parameters

Parameters	Value	Unit
Grid Frequency	Hz	60
Grid Voltage Peak Value	Volt	159
DG2 Transmission Resistance	0.05	Ohms
DG2 Transmission Inductance	1.5e-6	H
DG3 Transmission Resistance	0.15	Ohms

DG3 Transmission Inductance	4.5e-6	H
m_2	0.5*2*pi/600	
n_2	.5e-3	
m_3	0.5*2*pi/600	
n_3	.5e-3	
Virtual Resistance	5	
Connected Reactive Power	0	
Connected Active Load	1000	

Ouput

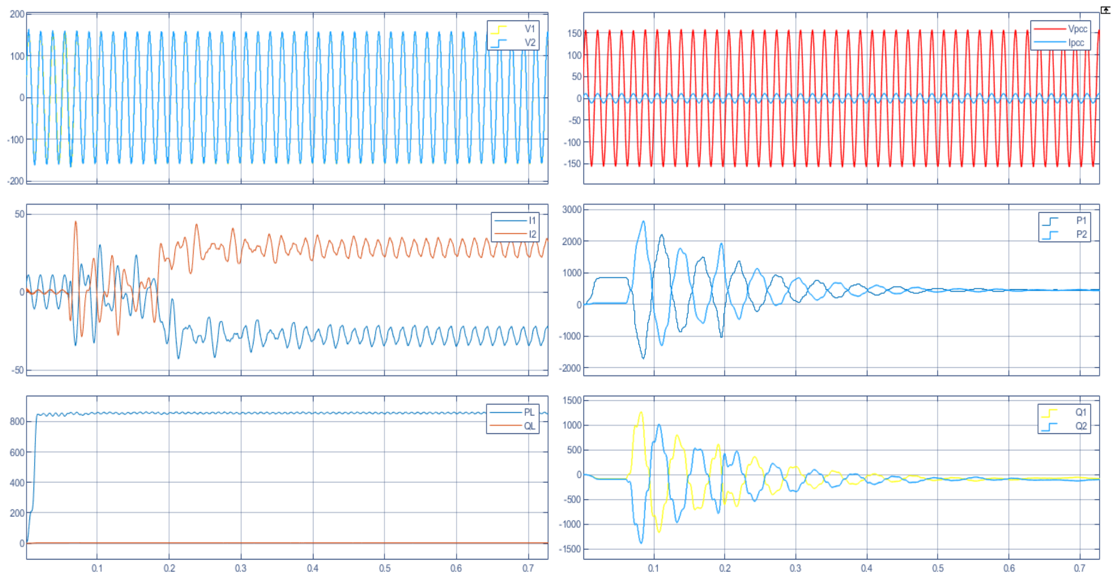

Figure 4.4: Large Virtual Resistance MATLAB/Simulink Model Output

We have found a stable grid frequency and voltage with proper active power-sharing, eliminating the tradeoff between grid voltage and power-sharing we observe in traditional droop control.

In this droop control, the transmission line impedances is not necessary to be measured as because a large virtual resistance is added on both DG, which makes the total virtual impendence close. But another problem of this design is the virtual voltage drop caused by large virtual resistance. In figure 4.4 the peak voltage is 150 V which is less than the reference 159 V. Due to zero crossing mismatch between DG2 and DG1, we monitor an initial turbulence before power sharing. We will use PLL to overcome this instability.

4.2.2 Negative Virtual Impedance Droop Control

To eliminate the grid voltage drop, we examine the negative virtual impedance droop control. We consider inverter one as a base impedance (which has the largest impedances) to calculate the other two DG's virtual impedances. In this droop control method, we can calculate the virtual impedances of inverter 2, 3 according to the equations (3.2.3),

$$Z_{v2} = Z_{l1} - Z_{l2} \tag{4.1}$$

$$Z_{v3} = Z_{l1} - Z_{l3} \tag{4.2}$$

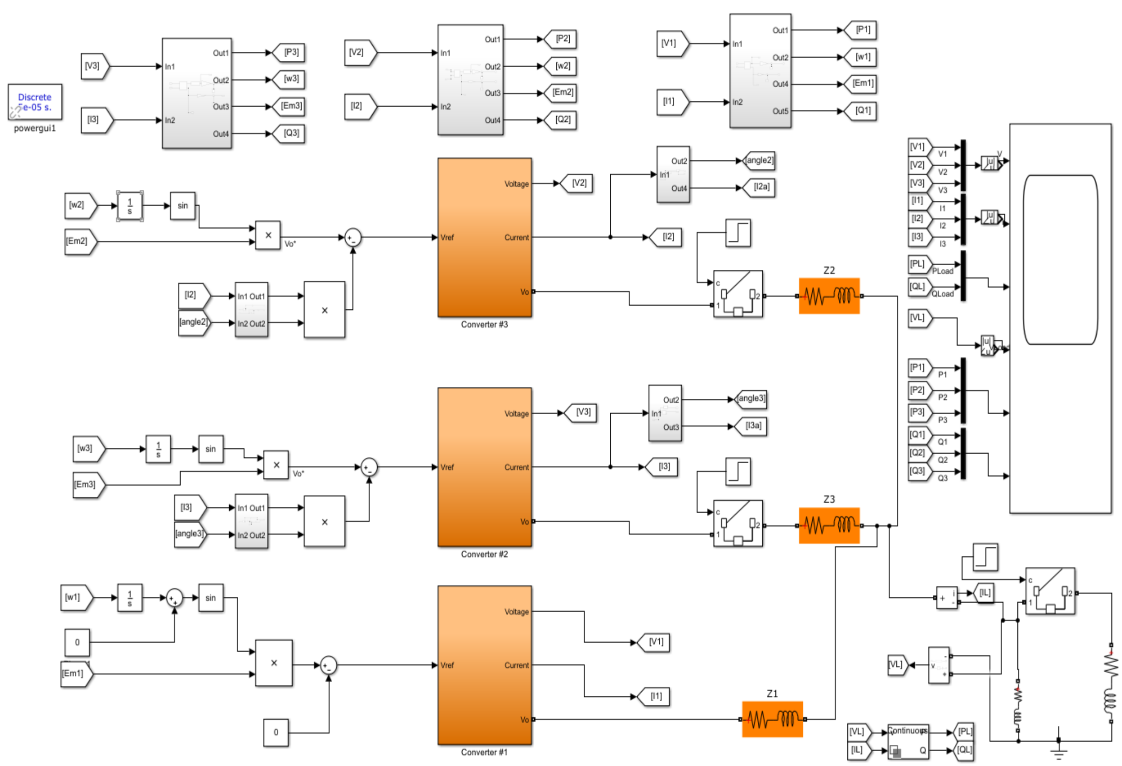

Figure 4.5: Virtual Impedance Droop Control MATLAB/Simulink Model

Simulation Parameters are listed in Table 4.3

Parameters	Value	Unit
DG1 Transmission Resistance	1.6	Ohms
DG1 Transmission Inductance	3e-4	H
DG2 Transmission Resistance	0.8	Ohms
DG2 Transmission Inductance	1.5e-4	H
DG3 Transmission Resistance	1.2	Ohms
DG3 Transmission Inductance	2.25e-4	H
DG 2 Virtual Resistance, Z_2	0.8+2*pi*60*1.5e-4i	Ohms
DG 3 Virtual Resistance, Z_3	0.4+2*pi*60*.75e-4i	Ohms
Connected Reactive Power	200	Watt
Connected Active Load	1000	Watt

Table 4.3 Virtual Impedance Droop Control MATLAB/Simulink Model Parameters

Simulation Output

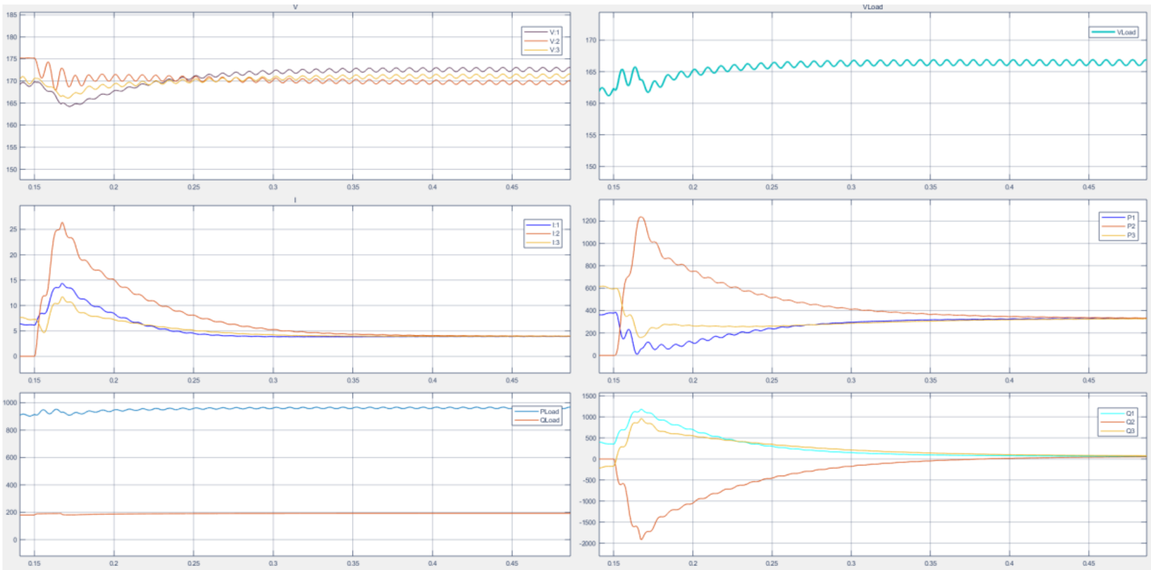

Figure 4.6: Virtual Impedance Droop Control MATLAB/Simulink Model Output

Using this droop control, we are able to get power-sharing without dropping large grid voltage according to the Simulink output as shown in Figure 4.6. We see an initial fluctuation due to zero-crossing mismatch when we connect inverter 2 and 3 into the grid. We have found the reactive power droop coefficient depends on the transmission line reactance. Also, the virtual impedance dependency on transmission line impedances makes this design impractical. Reactive power-sharing disrupts (in Figure 4.7) when we change the power factor of connected load unless we change the reactive power coefficient.

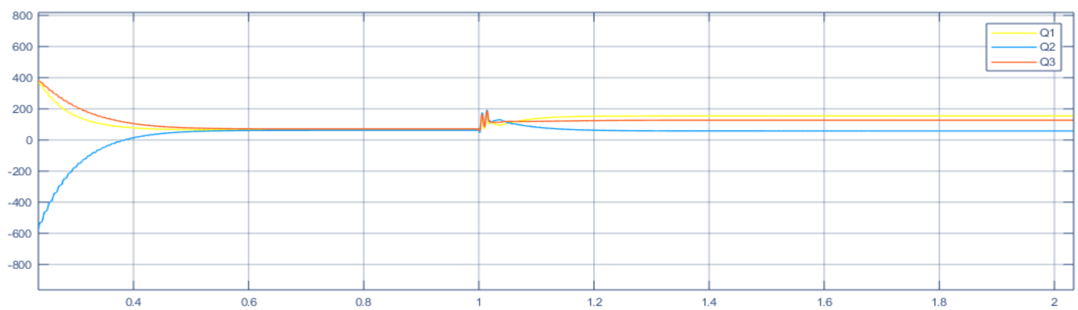

Figure 4.7: Disrupted Reactive Power Sharing when power factor of a load changes

To overcome the limitation of the power-sharing without degrading power quality in an islanded microgrid, this thesis suggests a two-layer V/F droop DG with other P/Q controlled DGs.

4.3 Designing the two-layer V/F control DG.

The first layer is like a conventional droop control, where voltage and frequency of the grid are controlled by active and reactive power. When the grid operates in an islanded mode, the VF DG will provide the necessary active and reactive power to the grid to make it stable. When there is a shortage of power, the grid voltage and frequency will be down. Simultaneously, the instantaneous power injection from the VF DG pushed grid frequency and voltage to a higher range.

When the demand power decrease, the grid frequency, and voltage increase. In this situation, the VF DG withdraws the grid's power instantaneously and decreases the grid frequency and voltage to a system rated label.

We took the idea from droop control P-V/Q-f in V/F DG as the transmission line is resistive. The second layer of the hierarchical control unit in VF DG will ensure the power-sharing without measuring the demand power.

4.3.1 VF Controlled Distributed Generator Flowchart in Grid

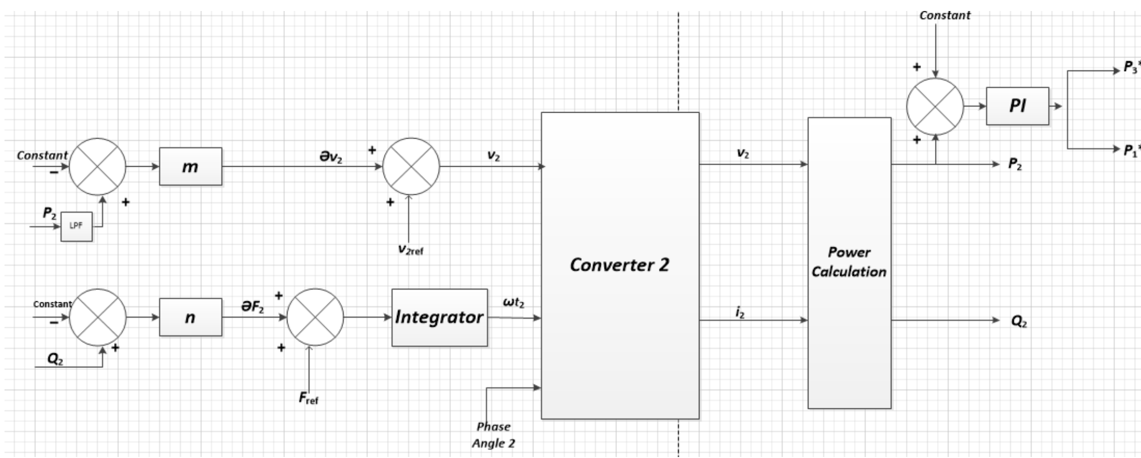

Figure 4.8: Two-layer VF control DG model

Inside the MATLAB/Simulink Model of VF DG

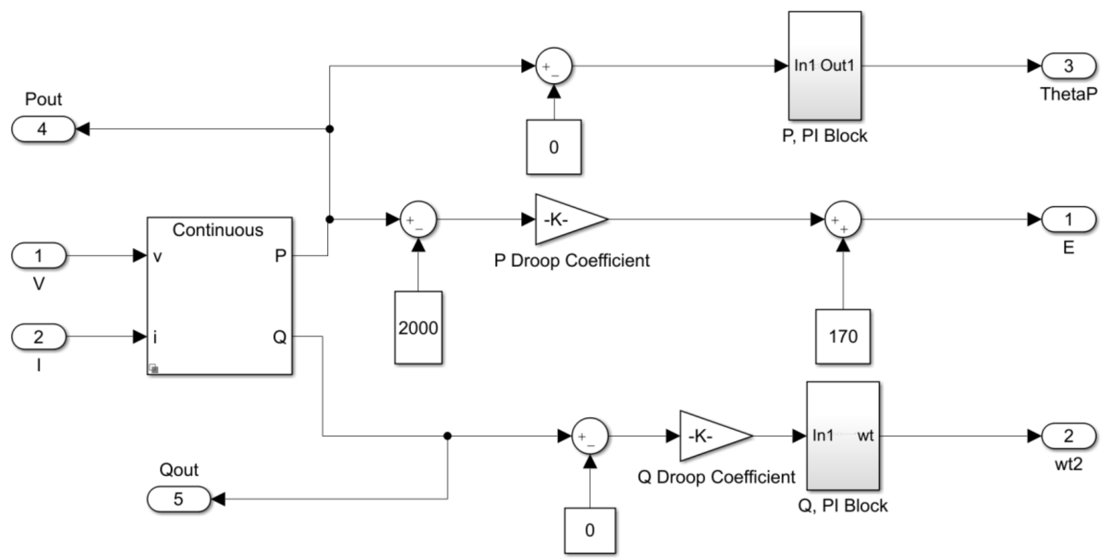

Figure 4.9: Inside the MATLAB/Simulink Model of VF DG

First layer is the P-V/Q-f droop control as transmission line is resistive. Active power droop coefficient is V_{ref} /9000, here 9000 is the maximum power capability. Here, 2000 in Figure 4.9 is the V/F control DG rated capability. Same reference setting goes for reactive power.

The second layer of the droop control will determine the gradient descent of the supplied power of V/F controlled DG into the grid. Later, this power supply will be provided by other PQ controlled DG. This second layer will determine the power shortage divergence. The portion of "ThetaP" in Figure 4.9, which will send back to other PQ controlled DGs based on fixed or dynamic weight, depends on the PQ DG design and its maximum capability.

4.3.2 PQ Controlled DG Designing

From chapter 3 equations 3.1.7-8, we can derive the power equations for resistive transmission line impedances as following

$$P \propto \delta \tag{4.3}$$

$$Q \propto V_{PCC} \tag{4.4}$$

Here, by using the equation of 4.3-3.4, the design of PQ DG is adopted. Two active and reactive power PI controller is used to maintain the constant power production, which create $\Delta\delta$ and ΔV based on the difference between the generation and reference power.

The PQ DG from Figure 4.10 is the same as before; only this time, we put dynamic power references to get the stable grid and proper power-sharing in islanded mode.

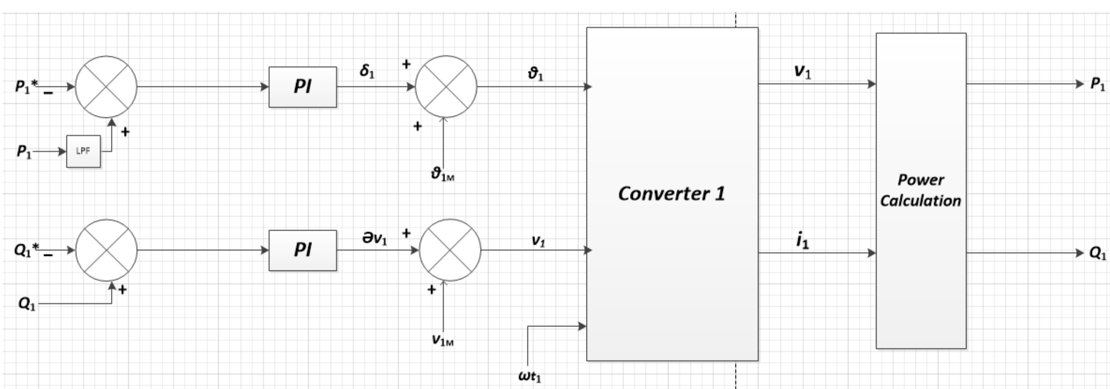

Figure 4.10: PQ Controlled DG Designing

4.3.3 Decentralized Two-layer VF DG integrating PQ DG

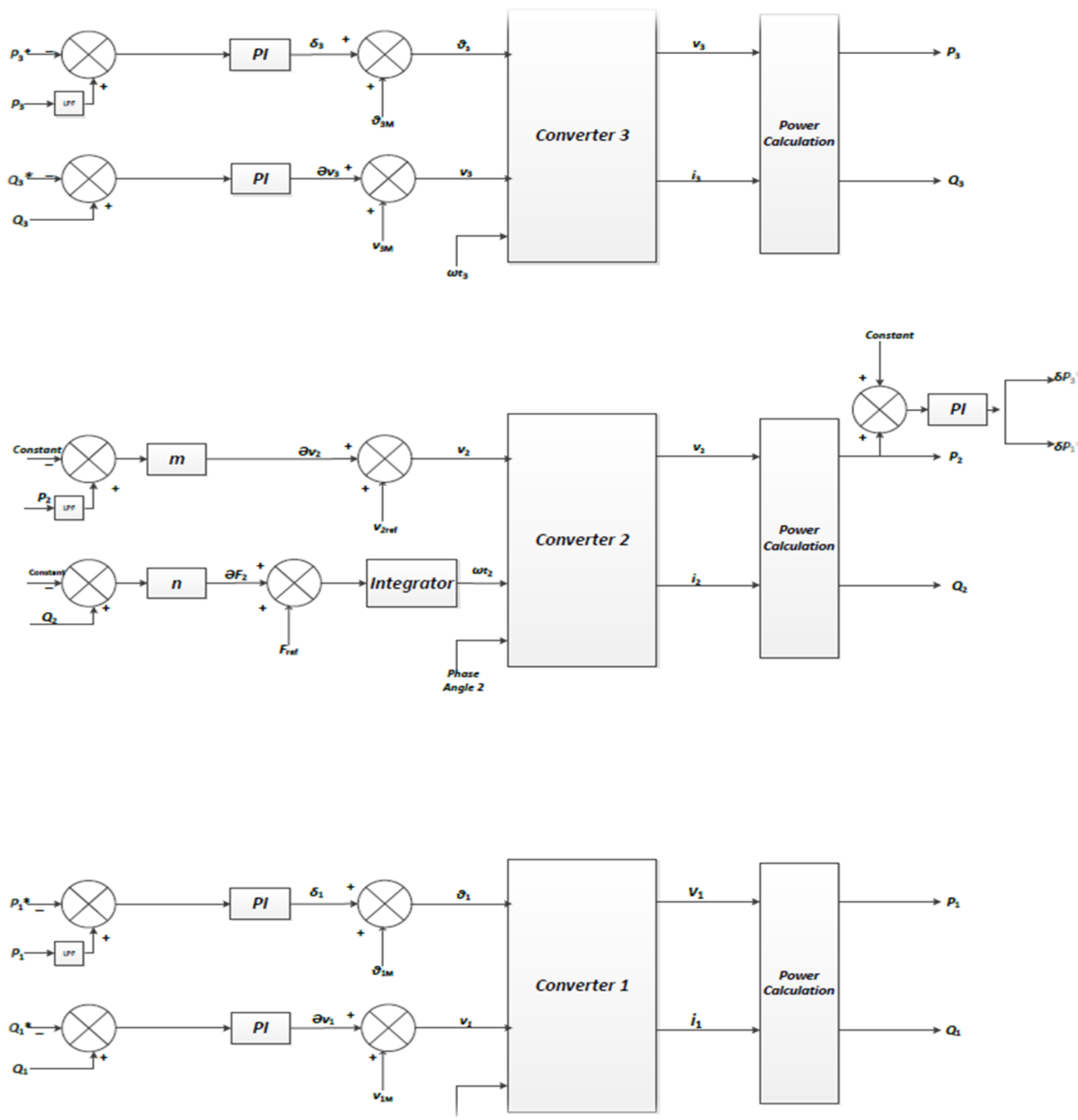

Figure 4.11: Decentralized Two-layer VF DG integrating PQ DG

Figure 4:11 illustrates the total flow chart of the decentralized islanded microgrid design using one VF DG and two PQ DG.

As described before, the power references for two PQ DGs will be slightly different from the previously adopted. In the islanded mode of microgrid, the power equations for two PQ DG will be,

$$P_1^* = P_1 - K_{1p} * \delta P_1^* \quad (4.5)$$

$$P_3^* = P_3 - K_{2p} * \delta P_3^* \quad (4.6)$$

$$Q_1^* = Q_1 - K_{1q} * \delta Q_1^* \quad (4.7)$$

$$Q_3^* = Q_3 - K_{2q} * \delta Q_3^* \quad (4.8)$$

In a stable grid with the following relation should maintain

$$K_{1p} + K_{2p} = 1 \quad (4.9)$$

$$K_{1q} + K_{2q} = 1 \quad (4.10)$$

$$\delta P_1^* + \delta P_3^* = P_2^* \quad (4.11)$$

$$\delta Q_1^* + \delta Q_3^* = Q_2^* \quad (4.12)$$

Where P_2^* is the supplied/withdraw active power of V/F DG. In case of the power injection, the value of the P_2^* will be positive. When V/F DG withdraw the power from grid, then the value of P_2^* and subsequently both $\delta P_1^*, \delta P_3^*$ will be negative.

Besides P_2^* and Q_2^*, other grid parameters $\omega t_1, \omega t_3, V_{1M},\ V_{3M}$ pass through different DGs to ensure the grid stability. Here, ωt will ensure the zero crossing when connect to the grid and reconnect to the grid.

Two typical cases were implemented in the MATLAB/Simulink for verifying the power sharing.

Case1:

In case of the value of $K_{1p} = 0.4$, $K_{2p} = 0.6$, we will get following output as shown on Figure 4.12.

Figure 4.12: Output In case of the value of $\mathrm{K_{1p}} = 0.4$, $\mathrm{K_{2p}} = 0.6$

Case 2:

When we put same power sharing ratio between two PQ DG, $K_{1p} = 0.5$, $K_{2p} = 0.5$, then will get the following scenario as Figure 4.13 shown

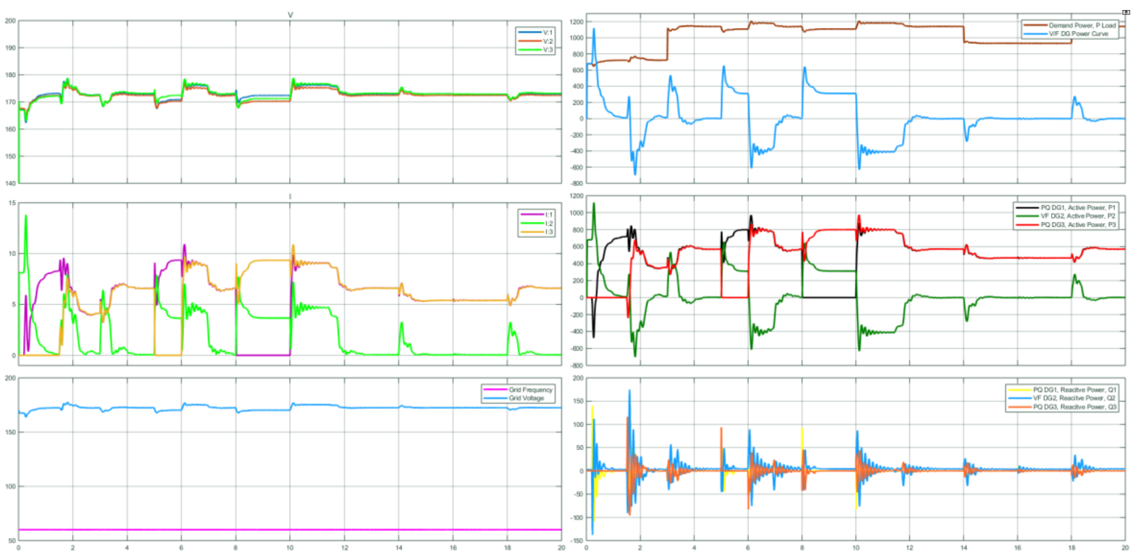

Figure 4.13: Output In case of the value of $K_{1\text{p}} = 0.5$, $K_{2\text{p}} = 0.5$

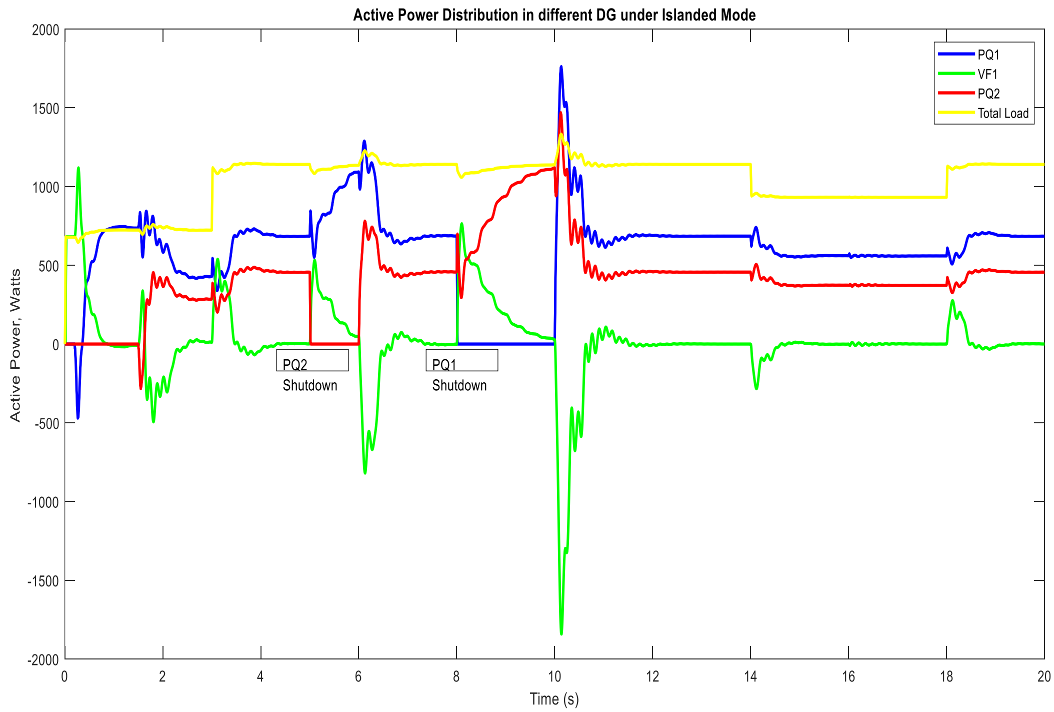

Figure 4.14: Explaining the power sharing in various intermittent nature of DG Demand power or connected load (yellow line) change over the time to investigate the grid stability. Green is considered VF1, whether blue is PQ1 and red is PQ2.

To minimize the initial fluctuations, the load should connect to the grid few seconds later after DG availability to the grid.

The simulations were conducted in the following sequences.

(1) at t=0s, only VF1 DG was connected to the grid at the beginning of simulation;

(2) at t=0.2s, PQ2 was connected to the grid

(3) at t=1.5s, PQ1 was connected to the grid

(4) at t=5s, PQ2 was completely shut down, VF1 provide the power

(5) at t=6s, PQ2 is turn on, VF1 withdraw the power from the grid

(6) at t=8s, PQ1 was completely shut down, VF1 provide the power

(7) at t=10s, PQ1 is turn on, VF1 withdraw the power from the grid

In Figure 4.14, we observe the maximum overshoot caused by the shutting down of DG. In maximum overshoot, the VF DG injects or withdraws about 2000 watt, which is the same as the VF DG's rated power. Using high power density ESS, system stability, and power-sharing will be ensured in a short time.

The microgrid voltage and frequency simulation results are shown in Figure 4.15-16

Grid Voltage

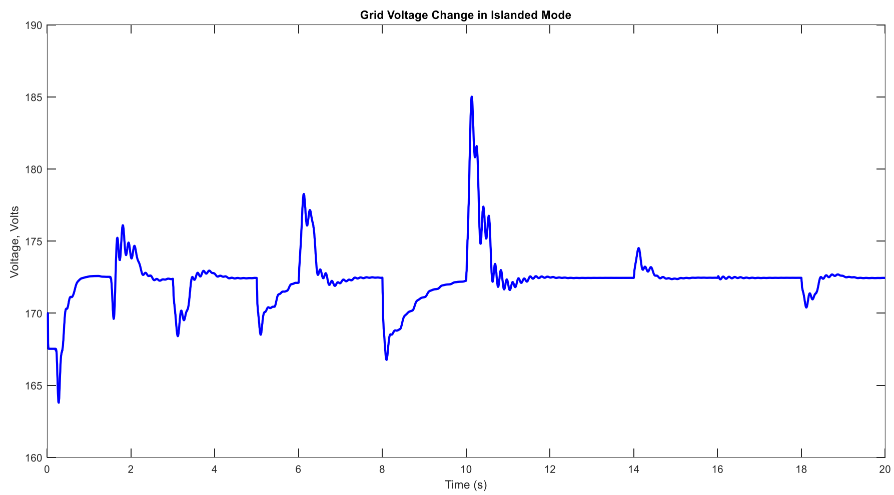

Figure 4.15: Grid Voltage

In figure 4.15, we have found a stable grid voltage even under extreme condition where one distributed generator completely shut down.

Grid Frequency in Islanded Mode

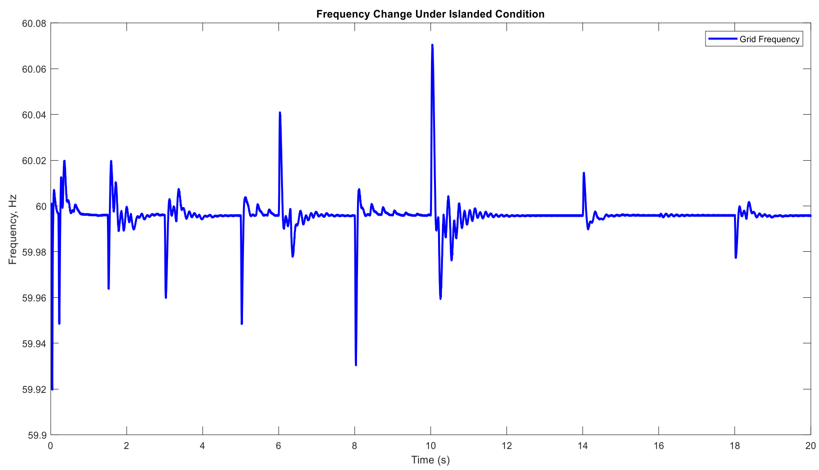

Figure 4.16: Grid Frequency

Grid frequency change from the range of 59.9-60.08 under various demand power and intermittent nature of DG. This grid frequency is extremely stable even one DG is completely shut down. We have found the maximum frequency deviation when DG1 is completely disconnected from the grid in figure 4.16.

4.4 Synchronizing two inverters using PLL

In controlled inverter synchronization scheme, the second inverter will get the phase and voltage magnitude as illustrated in figure 4.17.

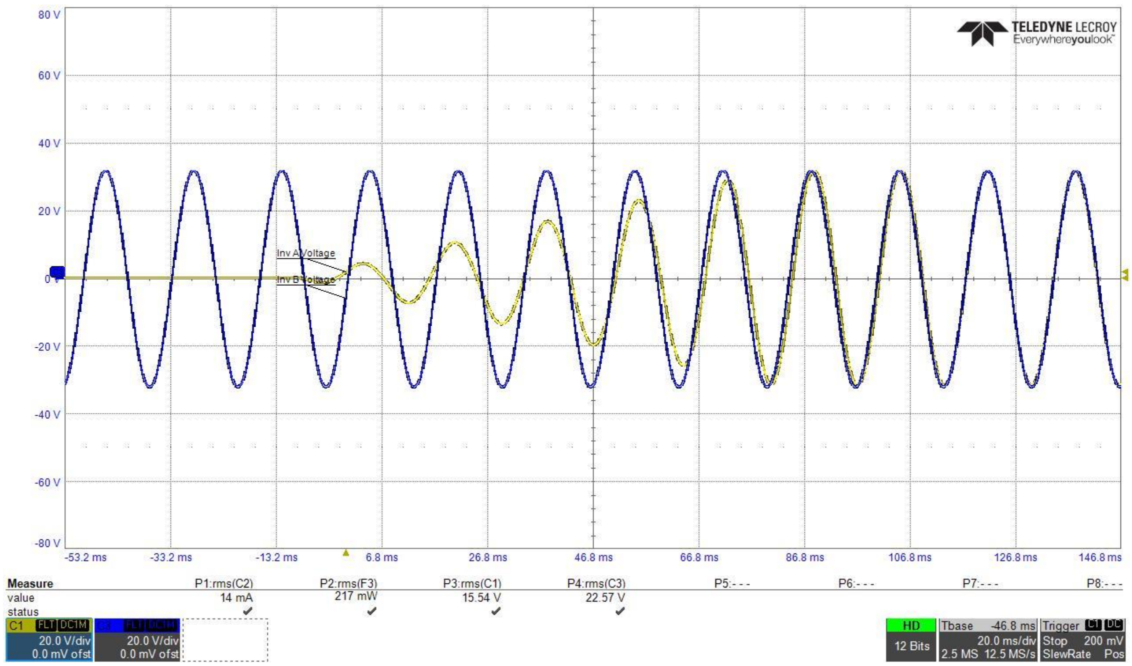

Figure 4.17: Inverter Synchronization Transient Response

As the second inverter might need both voltage magnitude and phase of the first inverter, we first transmit the positive and negative voltage references from the first inverter to the second inverter. Then we reconstruct the first inverter's output voltage in the second inverter to get the initial reference voltage (to minimize initial circulation current) and phase angle. This regenerated voltage passes through a phase-locked loop to extract the phase.

We might provide the same voltage references of different distributed inverters to minimize the initial turbulences when the inverter connects to a grid. In the case of voltage mismatch between DG, the circulation current tends to develop, ultimately increasing the grid's turbulences.

4.5 Power Sharing using Conventional Droop Control

After synchronizing inverter voltage, we implement the conventional droop control method to get the power sharing using the equations 3.1.11-12 between two DG inverters.

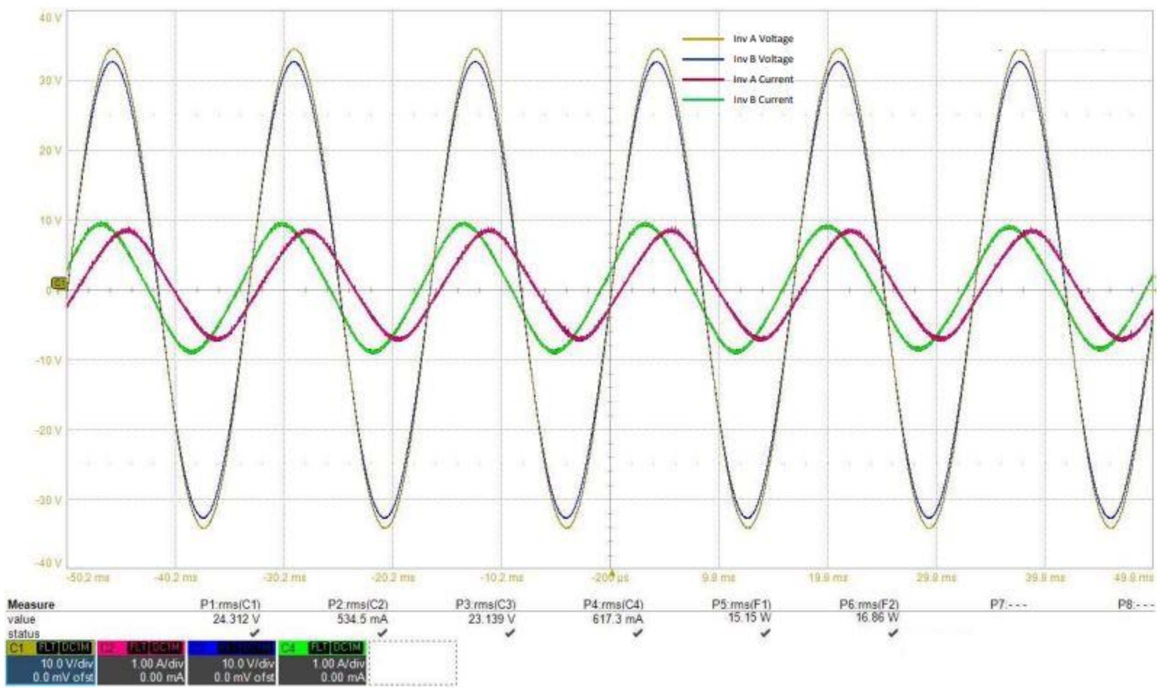

Figure 4.18: Two DG' inverters current and voltage by using conventional droop control

In Figure 4.18, we observe a phase shift of current in case of transmission line impedance mismatch between DG inverters and this phase shift depends on the line impedance difference. As discussed before in chapter three, we will be able to get the active power sharing as shown in Figure 4.18, but a phase shift of inverter current will create the circulation current into the grid.

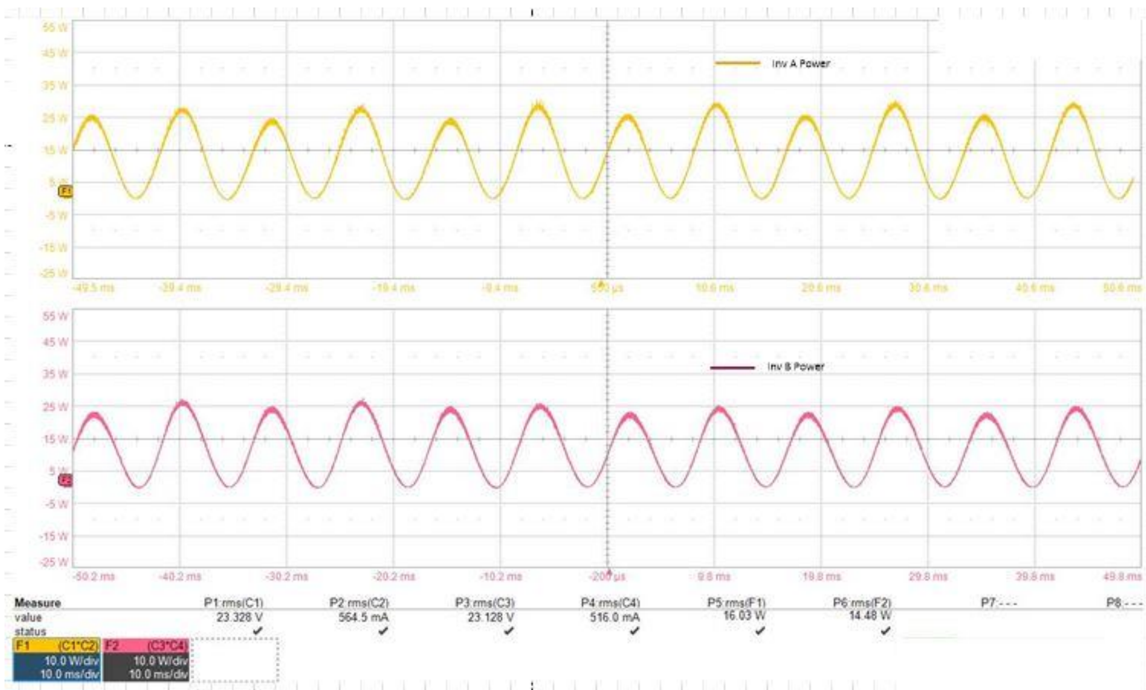

Figure 4.19: Power sharing between two DG' inverters in conventional droop control

From Figure 4.19, we observe instantaneous active power-sharing for resistive load. We have obtained the r.m.s value of these two inverters' active power generation is about 50W; by using the proper droop control coefficient, we can get ensure active power-sharing.

4.6 Power Sharing using Virtual Droop Control

Due to grid turbulences created by circulation current using conventional droop control, we implement the virtual droop control to get the power sharing. By using virtual droop control, we are able to synchronize both inverter current and voltage in case of transmission line impedance mismatch as shown in Figure 4.20.

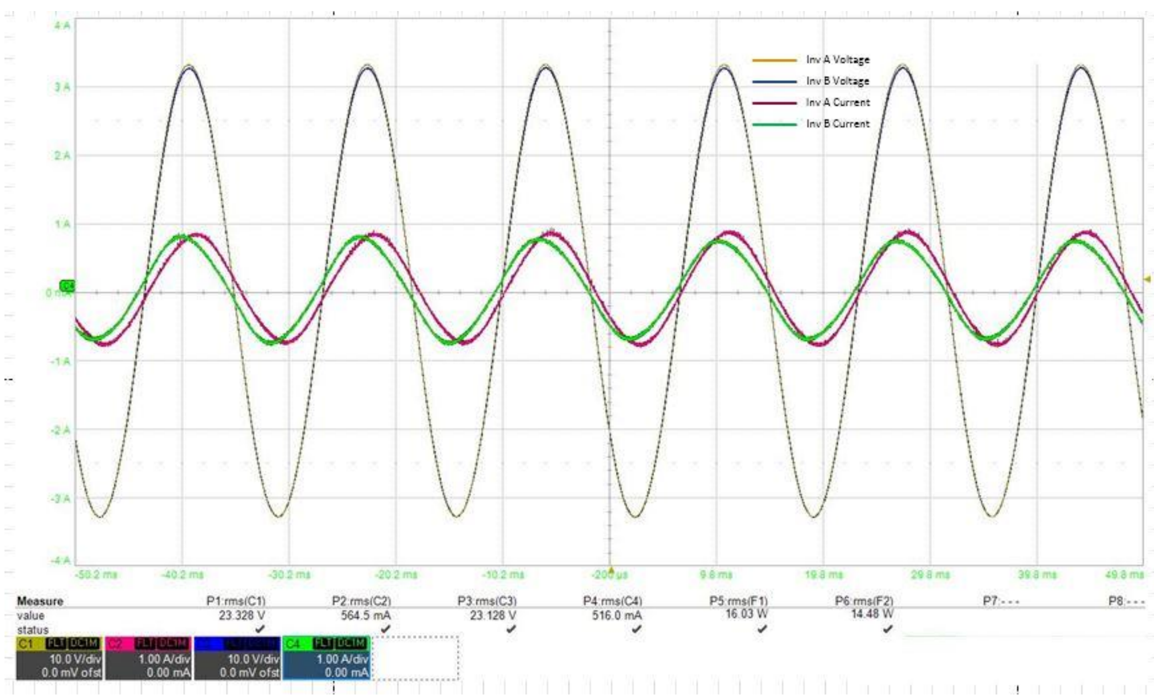

Figure 4.20: Two DG’ inverters current and voltage by using virtual droop control

By using this virtual droop control, the circulation current is minimized as well as proper power sharing among DG inverter as shown in Figure 4.21

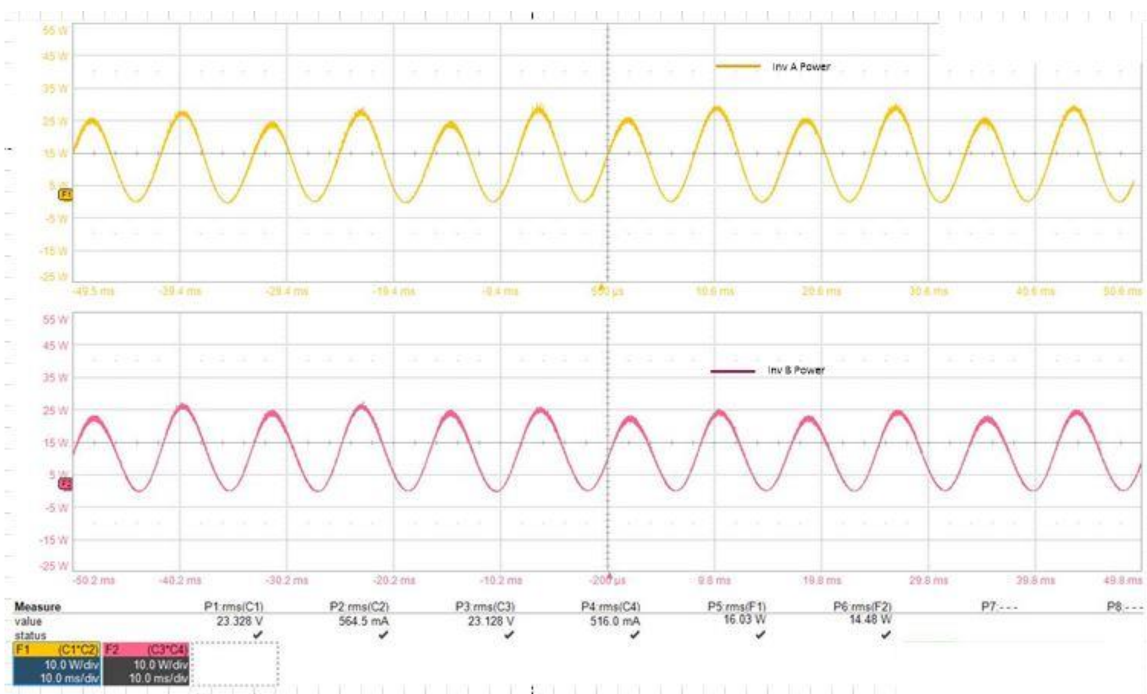

Figure 4.21: Power sharing between two DG' inverters in virtual droop control

4.7 Power Quality in Inverter Transient Response and Analyzing Third Harmonic Distortion

Maintaining the power quality during the inverter transition is important in microgrid. This section will analyze power quality inform of measuring the power sharing pattern and THD of current in transient response when the second inverter added in microgrid.

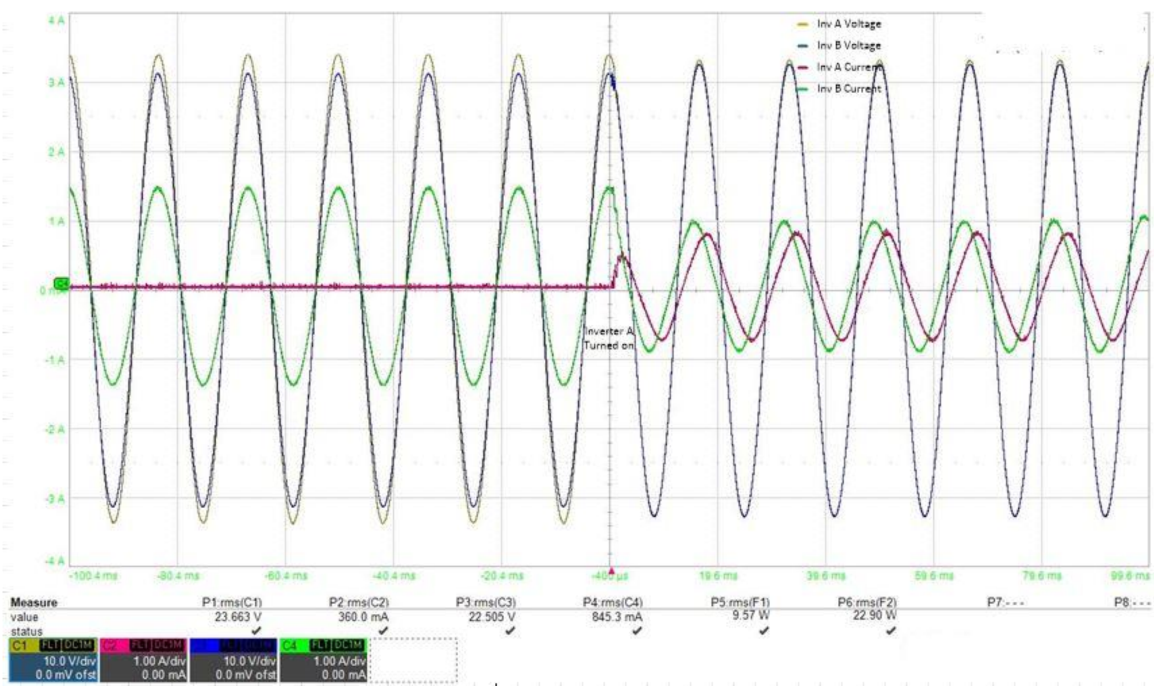

Figure 4.22: Transient response when Inv A added in microgrid.

In Figure 4.22 shows the transient response of both Inv A, B current and voltage, when inverter A is added into the microgrid. According to this figure, the microgrid maintain an smooth power sharing transition between these two inverters without disrupting both inverter current and voltage.

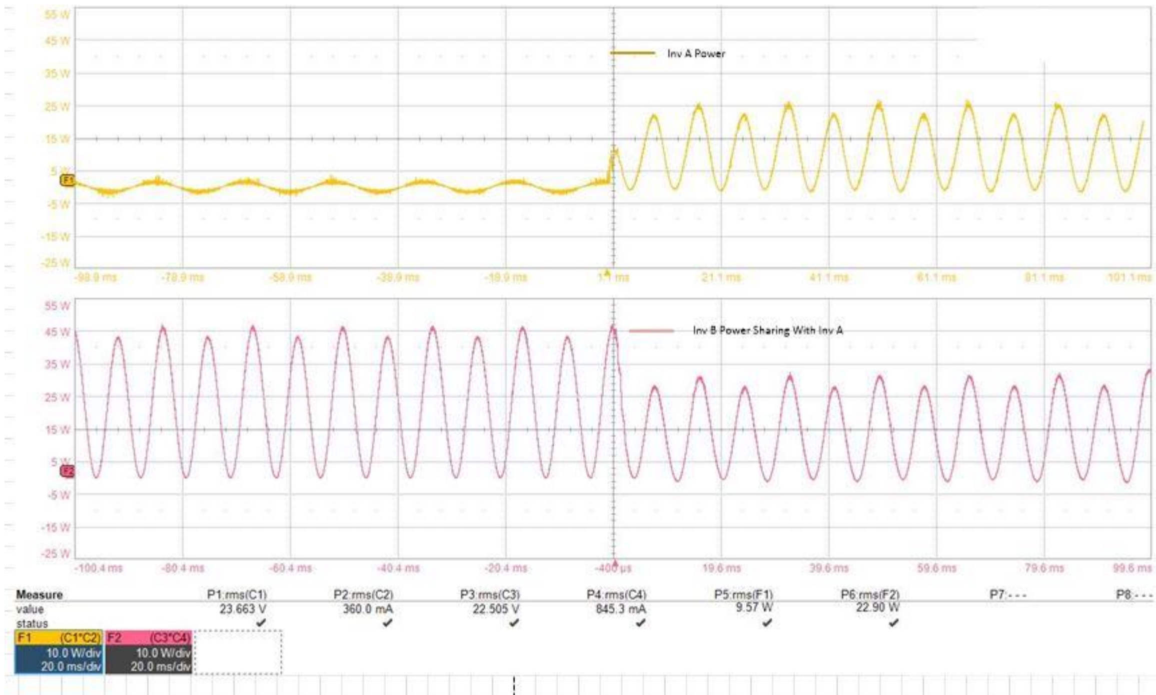

Figure 4.23: Power sharing under transient response

Figure 4.23 illustrates the power sharing pattern when Inv A is added to the microgrid. According to this figure, the microgrid almost instantaneously maintain smooth power sharing transition between two inverters.

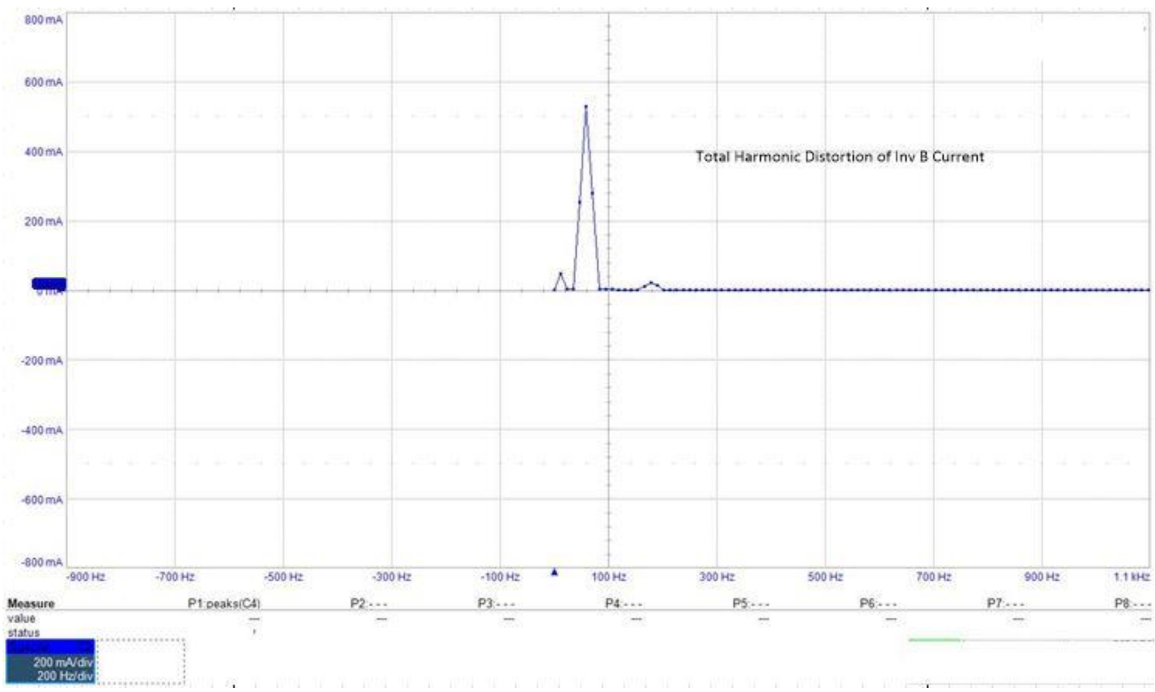

Figure 4.24: Third Harmonic Distortion of Inverter A Current.

Figure 4.24 illustrates the third harmonic distortion pattern of Inv A current. According to this oscilloscope spectrum analyzer figure of Inv A current, the third harmonic distortion current is almost minimized and under control for smooth power operation of microgrid.

Chapter 5. Conclusion and Recommendation for Future Work

This thesis exerted the concept from virtual impedance droop control, hierarchical secondary droop control for microgrid. The extensive communication used in the secondary control is mitigated, which measures the voltage and frequency fluctuation in terms of active and reactive power provided from the V/F controlled microgrid.

At first, the different operational modes of the microgrid is studied. In the grid-connected mode, the microgrid inertia is provided by the utility grid. With constant DG generated voltage and frequency approaching to grid frequency and voltage will maintain the grid-injected power quality and power-sharing among connected loads. In the islanded mode, several microgrid control approaches such as conventional droop control, large virtual impedance droop control, and decentralized V/F controlled microgrid are investigated.

There are some issue of the conventional droop control, one is the tradeoff between the active power-sharing and grid point of common coupling voltage (V_{PCC}) in conventional droop control, the other is the reactive power sharing could not obtain the transmission line impedance mismatch between the DGs. To overcome the limitation of conventional droop control, we investigate the virtual impedance droop control.

The active-reactive or PQ controlled distributed generators are simulated in MATLAB/Simulink. In grid connected mode, there is one DG controlled by a VF controller and the rest operate as a PQ controlled mode.

The simulation results show an active power and reactive power sharing while maintaining the grid frequency and voltage stable. When the connected-load power factor changes, the droop coefficient needs to be adjusted to maintain the proper power-sharing ratio. When the number of distributed generators is more than three, it is hard to obtain power-sharing as the connected load's power factor might change with time. Moreover, in the negative virtual impedance, the transmission line impedances need to be tracked, which is difficult as we know that the transmission line impedances change over time and depend on temperature or season changes. In this virtual droop control, the reactive power-sharing disrupts when we change the power factor of connected load unless we change the reactive power coefficient.

To overcome virtual droop control shortcomings, the decentralized two-layer V/F controlled microgrid is developed. In this microgrid communication network, the DG only exchanges the information with its neighbor DGs. In this decentralized communication network, a DG communicates with its neighbor DG to get the information such as voltage and phase angle. Using the first layer of V/F controlled, the proper power-sharing can be achieved under stable demand power. When we use the only first layer of V/F controlled DG, the grid has to exchange extensive information between DGs such as connected load, power generation.

The second layer of V/F control is developed to deal with the communication delay and data loss issue, i.e., the instantaneous power is measured and is sent to other PQ controlled DGs to update the power references based on their capability, which would take high variation in various form of voltage, frequency, demand power, power fluctuations. The V/F DG provides the necessary power even one of the DG power is not available.

In the experiment, we observe a circulation current when we implement the conventional droop control to get the power sharing. But by using virtual droop control, this circulation current is minimized as well as proper power sharing among DG' inverters.

Bibliography

[1] Lior, Noam. "Energy resources and use: The present situation and possible paths to the future." *Energy*, vol. 33, no. 6, pp. 842-857, 2008.

[2] Al-Ghussain, Loiy. "Global warming: review on driving forces and mitigation." *Environmental Progress & Sustainable Energy*, vol. 38, no. 1, pp. 13-21, 2019.

[3] Fonseca, M., Alves, L., Aguiar, A., Arai, E., Anderson, L., Rosan, T., Shimabukuro, Y. and Aragão, L., "Effects of climate and land-use change scenarios on fire probability during the 21st century in the Brazilian Amazon," *Global Change Biology*, vol. 25, no. 9, pp. 2931-2946, 2019.

[4] Omer, Abdeen Mustafa. "Energy, environment and sustainable development." *Renewable and sustainable energy reviews*, vol. 12, no. 9, pp. 2265-2300, 2008.

[5] Samad, Tariq, and Anuradha M. Annaswamy. "Controls for smart grids: Architectures and applications." *Proceedings of the IEEE*, vol. 105, no. 11, pp. 2244-2261, 2017.

[6] Singh, Alka, and Bhim Singh. "Power quality issues related to distributed energy source integration to utility grids." In *2010 Annual IEEE India Conference (INDICON)*, pp. 1-5, 2010.

[7] Bouzid, Allal M., Josep M. Guerrero, Ahmed Cheriti, Mohamed Bouhamida, Pierre Sicard, and Mustapha Benghanem. "A survey on control of electric power distributed generation systems for microgrid applications." *Renewable and Sustainable Energy Reviews*, vol. 44, pp. 751-766, Apr. 2015.

[8] Asif, Muhammad, and Tariq Muneer. "Energy supply, its demand and security issues for developed and emerging economies." *Renewable and sustainable energy reviews*, vol. 11, no. 7 pp. 1388-1413, 2007.

[9] Antoniadou-Plytaria, Kyriaki E., Iasonas N. Kouveliotis-Lysikatos, Pavlos S. Georgilakis, and Nikos D. Hatziargyriou. "Distributed and decentralized voltage control of smart distribution networks: Models, methods, and future research." *IEEE Transactions on smart grid*, vol. 8, no. 6, pp. 2999-3008, 2017.

[10] Huang, Qiyuan, Zhijie Wang, Jun Zhu, Dongwei Wang, and Bin Du. "Review on the Distributed Energy Storage Technology in the Application of the Micro Network." In *MATEC Web of Conferences*, vol. 22, pp. 02019, Jul. 2015.

[11] Tounsi, Asma, Hafedh Abid, and Khaled Elleuch. "On the wind energy conversion systems." In *Proc. IEEE 15th International Multi-Conference on Systems, Signals & Devices (SSD)*, pp. 1271-1279, 2018.

[12] Inthamoussou, Fernando A., Fernando D. Bianchi, Hernán De Battista, and Ricardo J. Mantz. "LPV wind turbine control with anti-windup features covering the complete wind speed range." *IEEE Transactions on Energy Conversion*, vol. 29, no. 1, pp. 259-266, 2014.

[13] Ibrahim, A., Raef Aboelsaud, and S. Obukhov. "Improved particle swarm optimization for global maximum power point tracking of partially shaded PV array." *Electrical Engineering,* vol. 101, no. 2, pp. 443-455, 2019.

[14] Meng, Wenchao, Xiaoyu Wang, and Shichao Liu. "Distributed load sharing of an inverter-based microgrid with reduced communication." *IEEE Transactions on Smart Grid*, vol. 9, no. 2, pp. 1354-1364, 2016.

[15] Li, Qiang, Feixiong Chen, Minyou Chen, Josep M. Guerrero, and Derek Abbott. "Agent-based decentralized control method for islanded microgrids." *IEEE Transactions on Smart Grid*, vol. 7, no. 2, pp. 637-649, 2015.

[16] Hajilu, N., G. B. Gharehpetian, S. H. Hosseinian, M. R. Poursistani, and M. Kohansal. "Power control strategy in islanded microgrids based on VF and PQ theory using droop control of inverters." In IEEE *2015 International Congress on Electric Industry Automation (ICEIA)*, pp. 37-42, 2015.

[17] Bayhan, Sertac, and Haitham Abu-Rub. "A simple control technique for distributed generations in grid-connected and islanded modes." In *IEEE 27th International Symposium on Industrial Electronics (ISIE)*, pp. 1237-1242, 2018.

[18] Pal, Shantanu, Michael Hitchens, and Vijay Varadharajan. "Towards the Design of a Trust Management Framework for the Internet of Things." In *13th International Conference on Sensing Technology (ICST)*, pp. 1-7, 2019.

[19] Pourbabak, Hajir, Tao Chen, and Wencong Su. "Centralized, decentralized, and distributed control for energy internet." In *The Energy Internet*, Woodhead Publishing, pp. 3-19, 2019.

[20] H. Han, X. Hou, J. Yang, J. Wu, M. Su and J. M. Guerrero, "Review of Power Sharing Control Strategies for Islanding Operation of AC Microgrids," in *IEEE Transactions on Smart Grid*, vol. 7, no. 1, pp. 200-215, 2016.

[21] Karimi, M., P. Wall, H. Mokhlis, and V. Terzija. "A new centralized adaptive underfrequency load shedding controller for microgrids based on a distribution state estimator." *IEEE Transactions on Power Delivery*, vol. 32, no. 1, pp. 370-380, 2016.

[22] Wang, Chengshan, Tianyu Zhang, Fengzhang Luo, Fangxing Li, and Yanzhang Liu. "Impacts of cyber system on microgrid operational reliability." *IEEE Transactions on Smart Grid*, vol. 10, no. 1, pp. 105-115, 2017.

[23] Zheng, Lei, Ning Lu, and Lin Cai. "Reliable wireless communication networks for demand response control." *IEEE Transactions on Smart Grid*, vol. 4, no. 1, pp. 133-140, 2013.

[24] Zheng, Lei, Simon Parkinson, Dan Wang, Lin Cai, and Curran Crawford. "Energy efficient communication networks design for demand response in smart grid." In *2011 International Conference on Wireless Communications and Signal Processing (WCSP)*, pp. 1-6, 2011.

[25] Liu, Shichao, Xiaoyu Wang, and Peter Xiaoping Liu. "Impact of communication delays on secondary frequency control in an islanded microgrid." *IEEE Transactions on Industrial Electronics*, vol. 62, no. 4, pp. 2021-2031, 2014.

[26] Rua, David, LF Moura Pereira, Nuno Gil, and JA Peças Lopes. "Impact of multi-microgrid communication systems in islanded operation." In *2nd IEEE PES International Conference and Exhibition on Innovative Smart Grid Technologies*, pp. 1-6, 2011.

[27] Elsayed, Medhat, Melike Erol-Kantarci, Burak Kantarci, Lei Wu, and Jie Li. "Low-Latency Communications for Community Resilience Microgrids: A Reinforcement Learning Approach." *IEEE Transactions on Smart Grid*, vol. 11, no. 2, pp. 1091-1099, 2019.

[28] Ramos-Paz, Serafin, Fernando Ornelas-Tellez, and J. Jesús Rico-Melgoza. "Robust Nonlinear Optimal Control for Voltage-Frequency and Active-Reactive Power Regulation in Microgrids." In *2019 North American Power Symposium (NAPS)*, pp. 1-6, 2019.

[29] Pal, Shantanu, Michael Hitchens, and Vijay Varadharajan. "Towards the Design of a Trust Management Framework for the Internet of Things." In *2019 13th International Conference on Sensing Technology (ICST)*, pp. 1-7, 2019.

[30] Ackermann, Thomas, Göran Andersson, and Lennart Söder. "Distributed generation: a definition." *Electric power systems research*, vol. 57, no. 3, pp. 195-204, 2001.

[31] Surprenant, Matthew, Ian Hiskens, and Giri Venkataramanan. "Phase locked loop control of inverters in a microgrid." In *IEEE Energy Conversion Congress and Exposition*, pp. 667-672, 2011.

[32] EPRI | Distributed PV Monitoring and Feeder Analysis, 2020.

[33] Rasheduzzaman, Md, and Jonathan W. Kimball. "Modeling and tuning of an improved delayed-signal-cancellation PLL for microgrid application." *IEEE Transactions on Energy Conversion*, vol. 34, no. 2, pp. 712-721, 2018.

[34] Abramovitch, Daniel. "Phase-locked loops: A control centric tutorial." In IEEE *Proceedings of the 2002 American control conference (cat. No. CH37301)*, vol. 1, no. *CH37301*, pp. 1-15, May. 2002.

[35] Chatterjee, Shamik, and V. Mukherjee. "PID controller for automatic voltage regulator using teaching–learning based optimization technique." *International Journal of Electrical Power & Energy Systems*, vol. 77, pp. 418-429, May, 2016.

[36] Al-Saedi, Waleed, Stefan W. Lachowicz, Daryoush Habibi, and Octavian Bass. "Power quality enhancement in autonomous microgrid operation using particle swarm optimization." *International Journal of Electrical Power & Energy Systems*, vol. 42, no. 1, pp. 139-149, 2012.

[37] Sedighizadeh, Mostafa, Masoud Esmaili, and Amir Eisapour-Moarref. "Voltage And Frequency Regulation In Autonomous Microgrids Using Hybrid Big Bang-Big Crunch Algorithm". *Applied Soft Computing*, vol. 52, pp. 176-189, Mar. 2017.

[38] Lopes, JA Peças, C. L. Moreira, and A. G. Madureira. "Defining control strategies for microgrids islanded operation." *IEEE Transactions on power systems*, vol. 21, no. 2, pp. 916-924, 2006.

[39] Gaonkar, D. N., and Josep M. Guerrero. "Improved Pf/QV and PV/Qf droop controllers for parallel distributed generation inverters in AC microgrid." *Sustainable cities and society*, vol. 41, pp. 421-442, Aug. 2018.

[40] Guan, Yajuan, Weiyang Wu, and Xiaoqiang Guo. "Control strategy for three-phase inverters dominated microgrid in autonomous operation." In *Zhongguo Dianji Gongcheng Xuebao(Proceedings of the Chinese Society of Electrical Engineering)*, vol. 31, no. 33, pp. 52-60, 2011.

[41] Yao, Wei, Min Chen, José Matas, Josep M. Guerrero, and Zhao-Ming Qian. "Design And Analysis Of The Droop Control Method For Parallel Inverters Considering The Impact Of The Complex Impedance On The Power Sharing". *IEEE Transactions On Industrial Electronics*, vol. 58, no. 2, pp. 576-588, 2011.

[42] Tayab, Usman Bashir, Mohd Azrik Bin Roslan, Leong Jenn Hwai, and Muhammad Kashif. "A review of droop control techniques for microgrid." *Renewable and Sustainable Energy Reviews*, vol. 76, pp. 717-727, 2017.

[43] Guerrero, Josep M., Juan C. Vasquez, José Matas, Luis García De Vicuña, and Miguel Castilla. "Hierarchical control of droop-controlled AC and DC

microgrids—A general approach toward standardization." *IEEE Transactions on industrial electronics*, vol. 58, no. 1, pp. 158-172, 2010.

[44] Guerrero, Josep M., Néstor Berbel, L. García de Vicuña, José Matas, Jaume Miret, and Miguel Castilla. "Droop control method for the parallel operation of online uninterruptible power systems using resistive output impedance." In *Twenty-First Annual IEEE Applied Power Electronics Conference and Exposition, APEC'06.*, pp. 7-pp, 2006.

[45] Skjellnes, Tore, Asle Skjellnes, and Lars E. Norum. "Load sharing for parallel inverters without communication." In *Nordic Workshop in Power and Industrial Electronics*, Aug. 2002.

[46] Zhang, Guowei, Zhihui Jin, Ningning Li, Xiao Hu, and Xisheng Tang. "A novel control strategy for parallel-connected converters in low voltage microgrid." In *2014 IEEE Conference and Expo Transportation Electrification Asia-Pacific (ITEC Asia-Pacific)*, pp. 1-6., 2014.

[47] Micallef, Alexander, Maurice Apap, Cyril Spiteri-Staines, Josep M. Guerrero, and Juan C. Vasquez. "Reactive power sharing and voltage harmonic distortion compensation of droop controlled single phase islanded microgrids." *IEEE Transactions on Smart Grid*, vol. 5, no. 3, pp.1149-1158, 2014.

[48] Rowe, Christopher N., Terrence J. Summers, Robert E. Betz, Timothy G. Moore, and Christopher D. Townsend. "Implementing the virtual output impedance concept in a three phase system utilising cascaded pi controllers in the dq rotating

reference frame for microgrid inverter control." In *IEEE 15th European Conference on Power Electronics and Applications (EPE)*, pp. 1-10, 2013.

[49] Li, Qiang, Feixiong Chen, Minyou Chen, Josep M. Guerrero, and Derek Abbott. "Agent-based decentralized control method for islanded microgrids." *IEEE Transactions on Smart Grid*, vol. 7, no. 2, pp. 637-649, 2015.

[50] Liu, Wei, Wei Gu, Wanxing Sheng, Xiaoli Meng, Zaijun Wu, and Wu Chen. "Decentralized multi-agent system-based cooperative frequency control for autonomous microgrids with communication constraints." *IEEE Transactions on Sustainable Energy*, vol. 5, no. 2, pp. 446-456, 2014.

[51] Gottwalt, Sebastian, Johannes Gärttner, Hartmut Schmeck, and Christof Weinhardt. "Modeling and valuation of residential demand flexibility for renewable energy integration." *IEEE Transactions on Smart Grid*, vol. 8, no. 6, pp. 2565-2574, 2016.

[52] Cominesi, Stefano Raimondi, Marcello Farina, Luca Giulioni, Bruno Picasso, and Riccardo Scattolini. "A two-layer stochastic model predictive control scheme for microgrids." *IEEE Transactions on Control Systems Technology*, vol. 26, no. 1, pp 1-13, 2017.